2miy

NASA TECHNICAL
MEMORANDUM

NASA TM X-64840

VEHICLE MISALIGNMENT PREDICTION AND
VEHICLE/EXPERIMENT POINTING
COMPATIBILITY ASSESSMENT

By J. D. Hoverkamp
Astronautics Laboratory

January 1974

NASA

George C. Marshall Space Flight Center
Marshall Space Flight Center, Alabama

NOTICE

Because of a waiver initiated and signed in compliance with NASA Policy Direc-
tive (NPD) 2220.4, para. 5-6, the International System of Units of Measurement
has not been used in this document.

ia

1. REPORT NO. NASA TM X-64840	2. GOVERNMENT ACCESSION NO.	3. RECIPIENT'S CATALOG NO.
4. TITLE AND SUBTITLE Vehicle Misalignment Prediction and Vehicle/Experiment Pointing Compatibility Assessment		5. REPORT DATE January 1974
		6. PERFORMING ORGANIZATION CODE
7. AUTHOR(S) J. D. Hoverkamp		8. PERFORMING ORGANIZATION REPORT #
9. PERFORMING ORGANIZATION NAME AND ADDRESS George C. Marshall Space Flight Center Marshall Space Flight Center, Alabama 35812		10. WORK UNIT NO.
		11. CONTRACT OR GRANT NO.
12. SPONSORING AGENCY NAME AND ADDRESS National Aeronautics and Space Administration Washington, D.C. 20546		13. TYPE OF REPORT & PERIOD COVERED Technical Memorandum
		14. SPONSORING AGENCY CODE

15. SUPPLEMENTARY NOTES

Prepared by Astronautics Laboratory, Science and Engineering

16. ABSTRACT

A technique for predicting vehicle misalignment, the relationship of vehicle misalignment to the total vehicle/experiment integration effort, and the methodology used in performing a vehicle/experiment pointing compatiblity assessment, are presented. The technique is demonstrated in detail by describing how it was used on the Skylab Program.

EDITOR'S NOTE

17. KEY WORDS Vehicle Misalignment Experiment Integration Compatibility Assessment Experiment Pointing Experiment Misalignment	18. DISTRIBUTION STATEMENT Unclassified-unlimited

19. SECURITY CLASSIF. (of this report) Unclassified	20. SECURITY CLASSIF. (of this page) Unclassified	21. NO. OF PAGES 72	22. PRICE NTIS

ACKNOWLEDGMENT

TABLE OF CONTENTS

LIST OF ILLUSTRATIONS

LIST OF TABLES

DEFINITION OF SYMBOLS

Symbol	Definition
A	Attitude control system accuracy
A_X A_Y A_Z	The component of A about the indicated axis
C	Attitude control system attitude bias capability
d	Diameter
E_{FOV}	Experiment sighting device field of view
M_B	Misalignment between two vehicle locations
M_E	Experiment misalignment
M_{EX} M_{EY} M_{EZ}	The component of M_E about the indicated axis
M_V	Vehicle misalignment
M_{VX} M_{VY} M_{VZ}	The component of M_V about the indicated axis

DEFINITION OF SYMBOLS (Concluded)

Symbol	Definition
P	Experiment pointing accuracy requirement
P_s	Experiment pointing accuracy requirements for simultaneous operations
r	Radius
θ	The specified angle in radians or degrees of arc

ABBREVIATIONS

ACD   Alignment control drawing

AM   Airlock Module

ATM   Apollo Telescope Mount

CSM   Command Service Module

DA   Deployment Assembly

EREP   Earth Resources Experiment Package

FAS   Fixed Airlock Shroud

FOV   Field of view

ICD   Interface control drawing

IU   Instrument Unit

JSC   Johnson Space Center

KSC   Kennedy Space Center

MDA   Multiple Docking Adapter

MDAC-WD   McDonnell Douglas Astronautics Company, Western Division

MMC   Martin Marietta Corporation

MSFC   Marshall Space Flight Center

OWS   Orbital Workshop

PS   Payload Shroud

RSS   Root sum square

ABBREVIATIONS (Concluded)

SAL   Scientific Airlock

UV   Ultraviolet

Z-LV   Z-local vertical

UNUSUAL TERMS

Basic Datum — A reference plane.

Beta — The smallest angle between the earth-sun line and the vehicle orbital plane.

Corollary Experiments — Skylab experiments not included in the ATM, medical, or EREP categories.

Nadir — The point where the local vertical intersects the surface of the earth.

Solar Inertial Attitude — The Skylab attitude defined as the Skylab X-axis in the orbital plane with the Z-axis coincident with the sun line.

ST-124 — The instrument unit guidance platform. Provided launch vehicle attitude control and Skylab attitude control until the ATM was activated.

Z-Local Vertical (Z-LV) Attitude — The Skylab attitude defined as the Skylab X-axis in the orbital plane with the Z-axis along the geodetic local vertical.

VEHICLE MISALIGNMENT PREDICTION AND VEHICLE/EXPERIMENT POINTING COMPATIBILITY ASSESSMENT

INTRODUCTION

With the advent of more application- or experiment-oriented missions and since candidate experiments for these missions will be increasing in both number and diversity, the area of vehicle/experiment integration will become increasingly important. One aspect of the experiment integration effort is the determination of pointing compatibility; that is, does the vehicle capability to accurately point an experiment at a selected target satisfy the requirements of the experiment? The three contributors to the vehicle pointing inaccuracies are (1) attitude control system uncertainties, (2) alignment differences between the control system and the experiments, and (3) alignment differences within the experiments. An alignment difference causes a pointing inaccuracy, since the experiment may be pointing in a direction different from the direction in which the control system believes the experiment is pointing. The relationship of vehicle alignment uncertainties to the experiment integration activity is shown in Figure 1.

The purpose of this document is to describe a technique for predicting vehicle alignment errors. The examples used are related exclusively to Skylab, since the technique was developed and used for Skylab. However, the technique described is also applicable to any future program in which a vehicle/experiment pointing compatibility analysis is required.

The term "vehicle" is used to mean the space vehicle that is the carrier of the experiments. The following terms are used synonymously in this document: alignment error and misalignment, and pointing accuracy and target acquisition accuracy. Examples of the Skylab experiment pointing accuracy requirements are given in Table 1.

The text will describe in detail: (1) the sources and types of alignment errors, (2) the technique for predicting misalignments, and (3) how the vehicle misalignments are used in pointing accuracy compatibility analyses for different types of experiments. The appendices provide examples of misalignment prediction and pointing accuracy compatibility analysis techniques by reviewing the work done for the Skylab program.
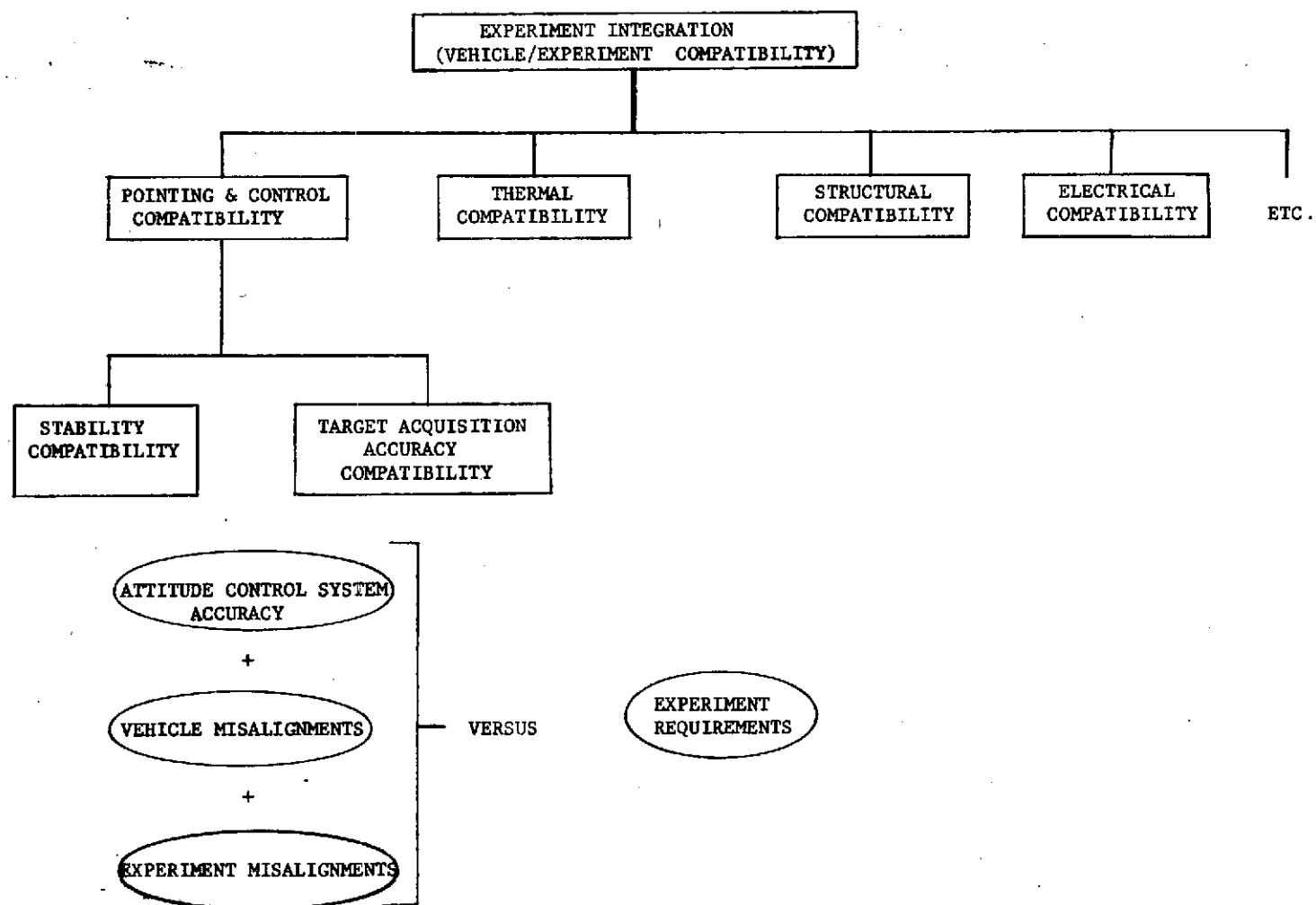
Figure 1. Relationship between vehicle misalignments and experiment integration.

TABLE 1. SELECTED SKYLAB EXPERIMENT POINTING

Experiment Number	Experiment Title	Target Requirements	Accuracy Requirements
S019	Ultraviolet (UV) Stellar Astronomy	Star Fields	± 0.5°
S020	X-Ray UV Solar Photography	Solar Disc	± 0.25°
S063	UV Ozone/Airglow Horizon Photography	Earth's Atmosphere	± 0.5° (post-flight knowledge)
S190A	Earth Resources - Multispectral Photographic Facility	Earth (Nadir)	± 2.5°
T025	Coronagraph Contamination Measurements	Solar Disc	± 0.5°
T027	Contamination Measurement	Miscellaneous Targets in Vicinity of Vehicle and Earth's Horizon	± 0.5° (post-flight knowledge)

The information presented in this document is based on the following assumptions:

1. General or representative experiment requirements and projected vehicle pointing accuracy capabilities were compared in the definition phases of the particular program in question.

2. As time passed, experiment requirements, the experiments themselves, or vehicle capabilities changed. This was due to better definition of requirements or capabilities, a change in mission or program objectives, or changes in the state-of-the-art of systems design.

3. A reanalysis or more detailed analysis of carrier/experiment compatibility was required.

The misalignment prediction technique described in this document is intended for use in the analysis mentioned in item 3 above.

VEHICLE MISALIGNMENT PREDICTION

The three sources of vehicle misalignments (M_V) are (1) structural misalignments, i.e., misalignments resulting from the manufacture and assembly processes, (2) thermal deflection (Fig. 2), and (3) dynamic effects or alignment errors due to the excitation of the structure by crew motion, thruster firings, or venting. Misalignments caused by dynamic effects warrant investigation but are generally negligible, since the magnitude of the structural excitation is relatively small.

There are two ways to treat alignment errors: as biases or uncertainties. A bias error would be a planned alignment offset or a measurement of the actual alignment. Uncertainties are predicted ranges of possible misalignments, e.g., the misalignment of the control system and a given experiment would be expressed as a bias plus or minus an uncertainty.

M_V, vehicle misalignment, can be determined during preflight by a number of methods. One is the measurement of the actual alignment of the control system and each concerned experiment. The advantage of this method is that the entire structural vehicle misalignment becomes a bias error (plus or minus the uncertainties associated with the measurement equipment or procedure). However, the possible thermal deflections must still be calculated and treated as uncertainties. This method, expensive in terms of time and equipment, is generally impractical.

EARTH

Thermal
Deflection
Misalignment

Expt

Control
System

SUN
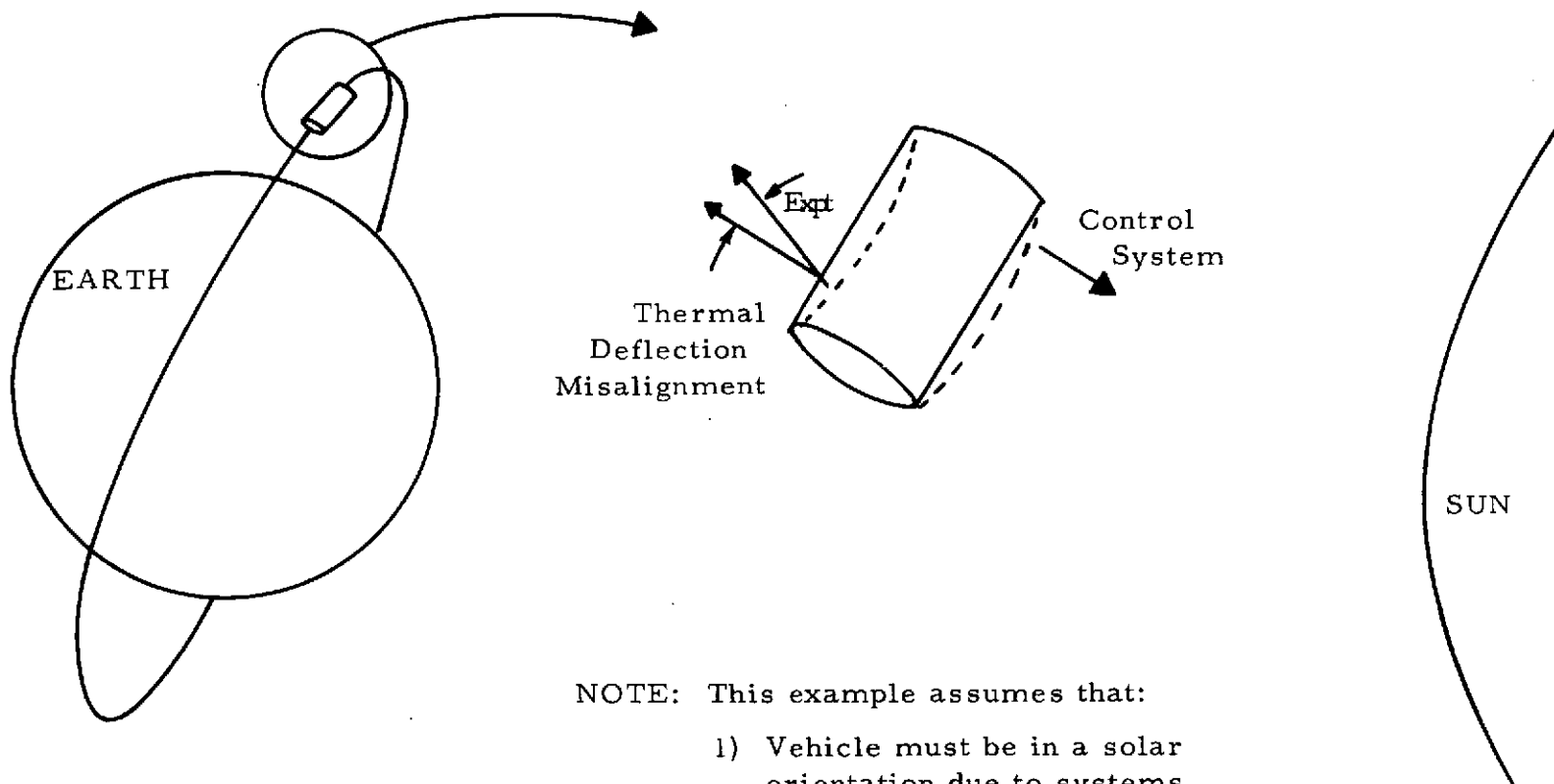
NOTE: This example assumes that:

1)   Vehicle must be in a solar
     orientation due to systems
     requirements and
2)   Experiment targets are stellar

Figure 2.   Example of thermal deflection misalignment.

Another means of alignment error determination is the alignment measurement of major vehicle subassemblies. This method costs less than a complete measurement for each experiment. Also, there is less bias and more uncertainty error with this method, since the individual measurements must be analytically combined.

A third method of preflight vehicle misalignment determination is to analytically determine the entire error using alignment control, manufacturing, assembly, and interface control drawings, or alignment specifications. This method is the least expensive but also the least desirable from an experiment integration point of view since the entire error is in the form of an uncertainty.

Thus, the problem in choosing a method of preflight alignment determination is that biases are preferred but more expensive to obtain. The best approach is a combination of the second and third methods discussed, i.e., the measurement of some alignments and the calculation of others. Those alignments to be measured are chosen based on the cost of the measurement and the relative importance of the particular alignment in the compatibility analysis.

This combination approach requires a conservative, yet realistic, means of calculating the alignment error components and combining them to obtain a vehicle misalignment. Conservatism is required to ensure compatibility with some factor of safety. Realism is required; otherwise, compatible experiments might be determined to be incompatible, costly changes might be made, or the experiment might be deleted from the program

The recommended alignment prediction technique is as follows (note: calculate and use alignment errors in the form of pure rotations about the vehicle axes and analyze each axis separately):

1. Calculate, or obtain from structural specialists, worst-case structural misalignments from drawings and specifications (Appendix A).

2. Assume that structural misalignments have a uniform frequency distribution. This will result in a more conservative calculated misalignment than would be obtained by assuming a normal frequency distribution. However, the result will be much more realistic than it would be if worst-case misalignments were added directly.

Frequency of Alignment Error

Magnitude of Alignment Error

-Uncertainty   +Uncertainty
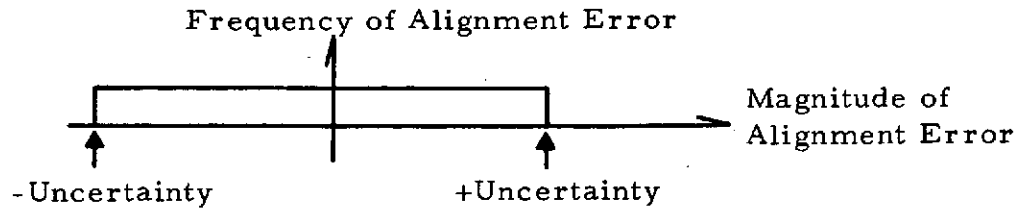
3. Calculate, or obtain from thermal and structural specialists, thermal deflection misalignments for "hot" and "cold" cases in various attitudes (Appendix A).

4. Assume that thermal deflection misalignment has a uniform frequency distribution with the hot and cold case misalignments as the end points.

Frequency of Error

Magnitude of Error
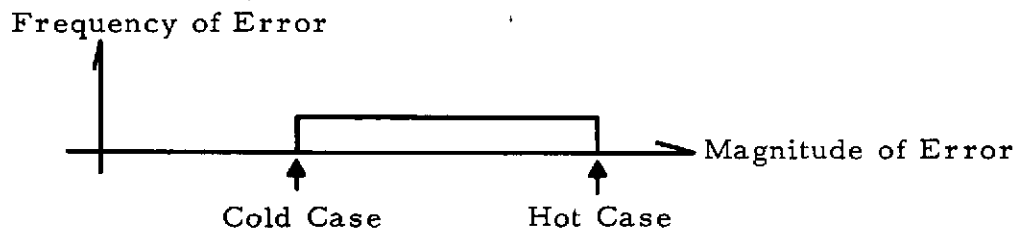
Cold Case   Hot Case

"Move" the distribution so that its midpoint is zero, and create a bias error = (cold case error + hot case error)/2.

5. Calculate, or obtain from structural specialists, the misalignment due to vehicle dynamic responses to crew motion and other disturbances (Appendix A, Reference 1, and an MSFC memorandum[1]).

6. Assume that dynamic misalignments also have a uniform frequency distribution with the maximum misalignments as the end points.

7. Obtain vehicle misalignment bias by adding the component biases.

8. Use a Monte Carlo technique (see source program in Appendix B) to combine uncertainty errors (uniform frequency distributions).

1. J. H. Farrow, Dynamic Effects on Skylab Misalignments, Memorandum S&E-ASTN-ADL(71-76), Marshall Space Flight Center, Marshall Space Flight Center, Ala., Sept. 7, 1971.

The total bias error ± the total uncertainty (in cumulative distribution form) can now be input to the compatibility analysis.
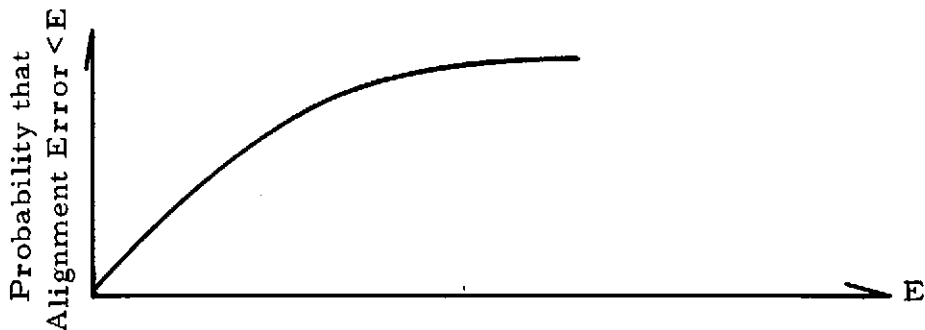
Thus the compatibility analyst can associate a probability with the uncertainty for vehicle misalignments that is consistent with the other compatibility analysis inputs.

Appendix A demonstrates the development of the component Skylab misalignments. Appendix B demonstrates the total Skylab misalignment prediction technique.

VEHICLE/EXPERIMENT POINTING COMPATIBILITY

The relationship of misalignments, pointing accuracy compatibility, and experiment integration was shown in Figure 1. The technique required to perform the pointing compatibility analysis is given in Figure 3. The compatibility analysis procedure only is shown, not the entire experiment integration procedure. For example, if the analysis determines that a certain experiment is incompatible, the experiment integration effort would continue until experiment or vehicle modifications were made or the experiment was deleted from the program.

The proper equation to use in the vehicle/experiment compatibility analysis depends on whether the experiment pointing can be determined in flight. For example, if a crew member will be able to look through a sighting device on the experiment and determine the actual experiment pointing, then, in the preflight analysis, equation (1) must be satisfied for compatibility to exist.
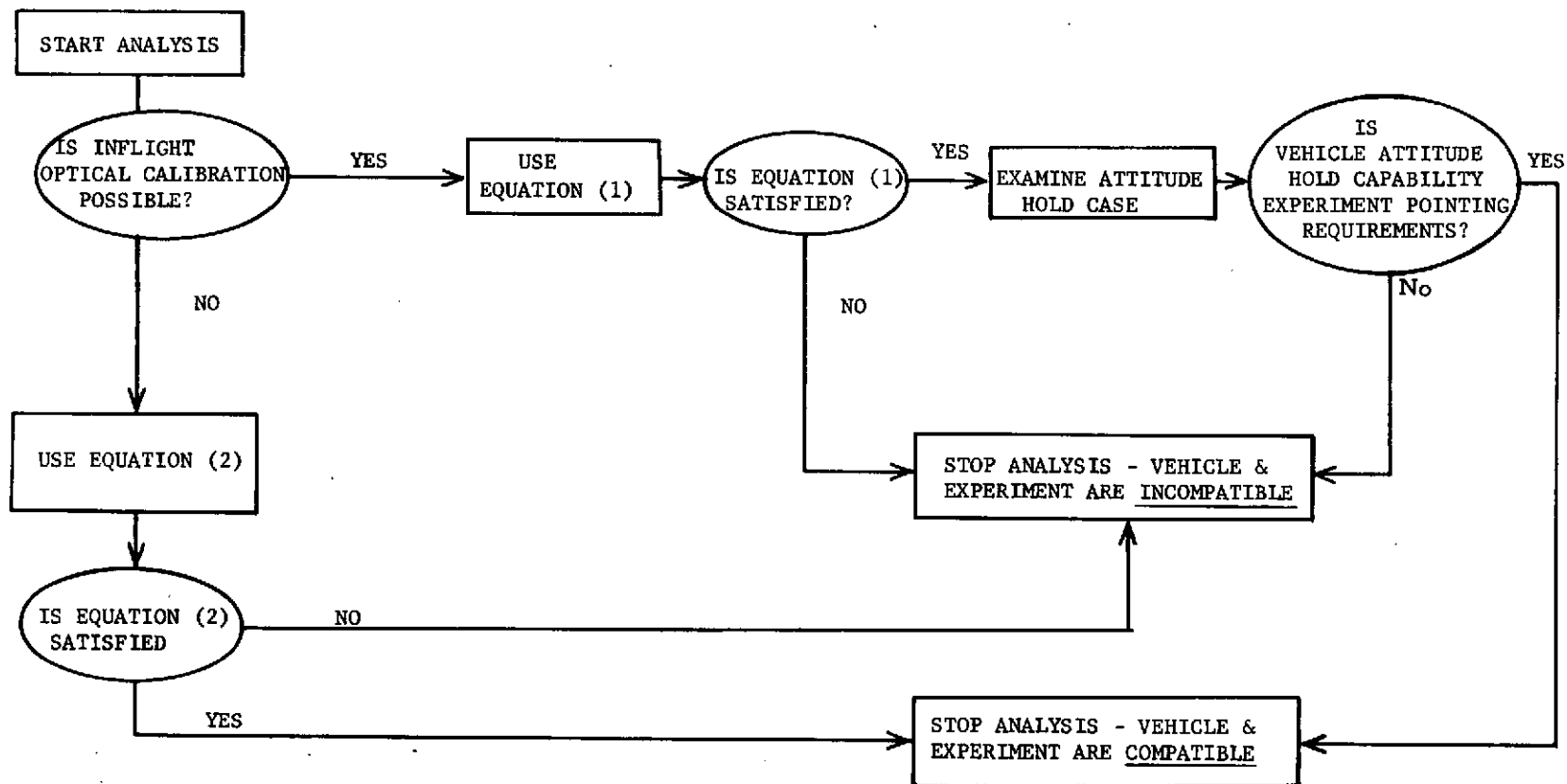
Figure 3. Vehicle/experiment pointing compatibility analysis procedure.

$$A + M_V + M_E \leq E_{FOV} \text{ or C (whichever is smaller)} \tag{1}$$

where

A = attitude control system pointing accuracy uncertainties,

M_V = vehicle misalignment,

M_E = experiment misalignment,

E_{FOV} = field of view of the experiment sighting device,

and

C = attitude offset capability of the control system.

C is determined by the attitude control system design or vehicle systems operating limitations; e.g., the attitude control thruster propellant usage in a nonstandard attitude or electrical power production from solar arrays in a non-standard solar attitude would limit the attitude offset capability of the vehicle. Both C and E_{FOV} will probably be considerably larger than the experiment pointing accuracy requirement. This is the advantage in having a sighting device to determine where the experiment is pointing. If equation (1) is satisfied, the attitude control system ability to hold a specified attitude must be less than the experiment pointing accuracy requirements for vehicle/experiment compatibility to exist. If, in addition, the experiment pointing is adjustable within the experiment, the allowable adjustment may replace C in equation (1).

If $E_{FOV} <$ C, the vehicle pointing accuracy uncertainties must be less than E_{FOV} or the crew member using the sighting device might not see the target. Target acquisition maneuvers of the vehicle under these conditions are not practical, especially if there is doubt as to the actual target pointing required. If C $< E_{FOV}$, the target could be seen but not acquired because of the limitations which initially set C.

10

If no in-flight optical experiment pointing calibration capability exists, equation (2) must be satisfied for compatibility to exist.

$$A + M_E + M_V \leq P \tag{2}$$

where A, M_E, and M_V are as defined for equation (1), and P is the experiment pointing accuracy requirement.

An example of special experiment pointing requirements is the requirement of two experiments in different vehicle locations to simultaneously acquire the same target. Assuming that either of the experiments satisfies equation (1) or (2), the following equation must also be satisfied for compatibility to exist:

$$M_B \leq P_S \tag{3}$$

where M_B is the possible alignment error between experiments, and P_S is the simultaneous experiment pointing accuracy requirements.

The use of equations (1), (2), and (3) to test for compatibility is demonstrated in Appendix C.

CONCLUSIONS

The vehicle misalignment is a significant input to the experiment/vehicle compatibility analysis. Prediction of these misalignments is often required, since a complete alignment measurement is often impossible or impractical. In addition, certain misalignments, e.g., thermal deflections, cannot be measured before flight. Thus, a misalignment prediction technique was developed for the Skylab program.

The comparison of predicted misalignments and Skylab misalignment data is presented in Appendix D. This comparison indicates that the technique for misalignment prediction presented in this report is somewhat conservative,

i.e., the predicted misalignments are greater than the flight misalignment data. However, this was expected and should not pose a problem in future programs unless a large number of potential experiments are "borderline" with respect to pointing compatibility. If that is the case, new, less conservative techniques should be investigated to predict misalignments and, in turn, determine the vehicle/experiment compatibility status.

APPENDIX A

SKYLAB ALIGNMENT ERROR COMPONENTS

This appendix describes the determination of the component Skylab misalignments. Figure A-1 shows the general Skylab orbital configuration including the reference coordinate system. Figures A-2 and A-3 describe the reference locations used in the analysis and details of the IU to MDA area, respectively. The component misalignments are listed in Table A-1. Figure A-4 and Table A-2 show the reference scheme for thermal deflections and the predicted deflections, respectively.

Note ⚠️ ATM EXPERIMENT OPTICAL SURFACE TO ATM BASIC DATUM

References 2 and 3 contain the ATM prelaunch alignment requirements. In addition, Reference 2 contains orbital alignment requirements. The orbital requirements represented larger misalignments and were used in this study.

The misalignment of the ATM experiment optical axis and the ATM fine sun sensor (FSS) was used to represent the misalignment of the experiment optical axis and the ATM basic datum. The alignment error of the FSS to the basic datum is included in the control system errors not addressed in this appendix.

The misalignment of S052 and the FSS was found to be the worst case after a survey of all the ATM experiment/FSS alignments.

From Reference 2 for S052 to FSS:

$$M_{VX} = \pm 0 \text{ deg, } 3 \text{ min} = 0.0 \pm 0.050 \text{ deg,}$$

$$M_{VY} = \pm 0 \text{ deg, } 3 \text{ min} = 0.0 \pm 0.050 \text{ deg,}$$

$$M_{VZ} = \pm 1 \text{ deg} = 0.0 \pm 1.0 \text{ deg.}$$
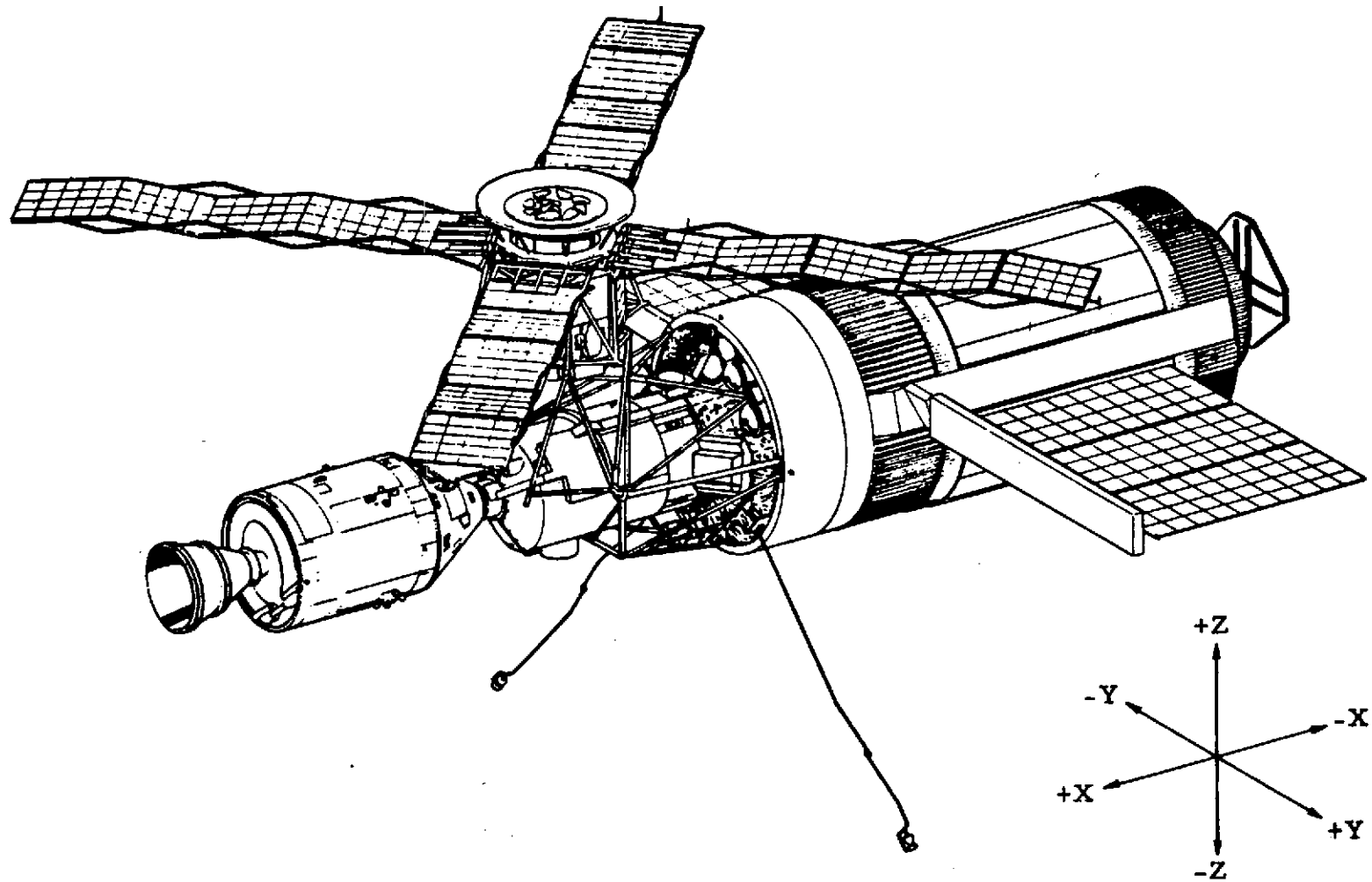
Figure A-1. General configuration — dynamic body axis reference system.

ATM

EXPERIMENTS

ATM BASIC DATUM
ATM/DA INTERFACE

SOLAR SAL

S194

S190
S191
S192

S193

ANTI-SOLAR SAL
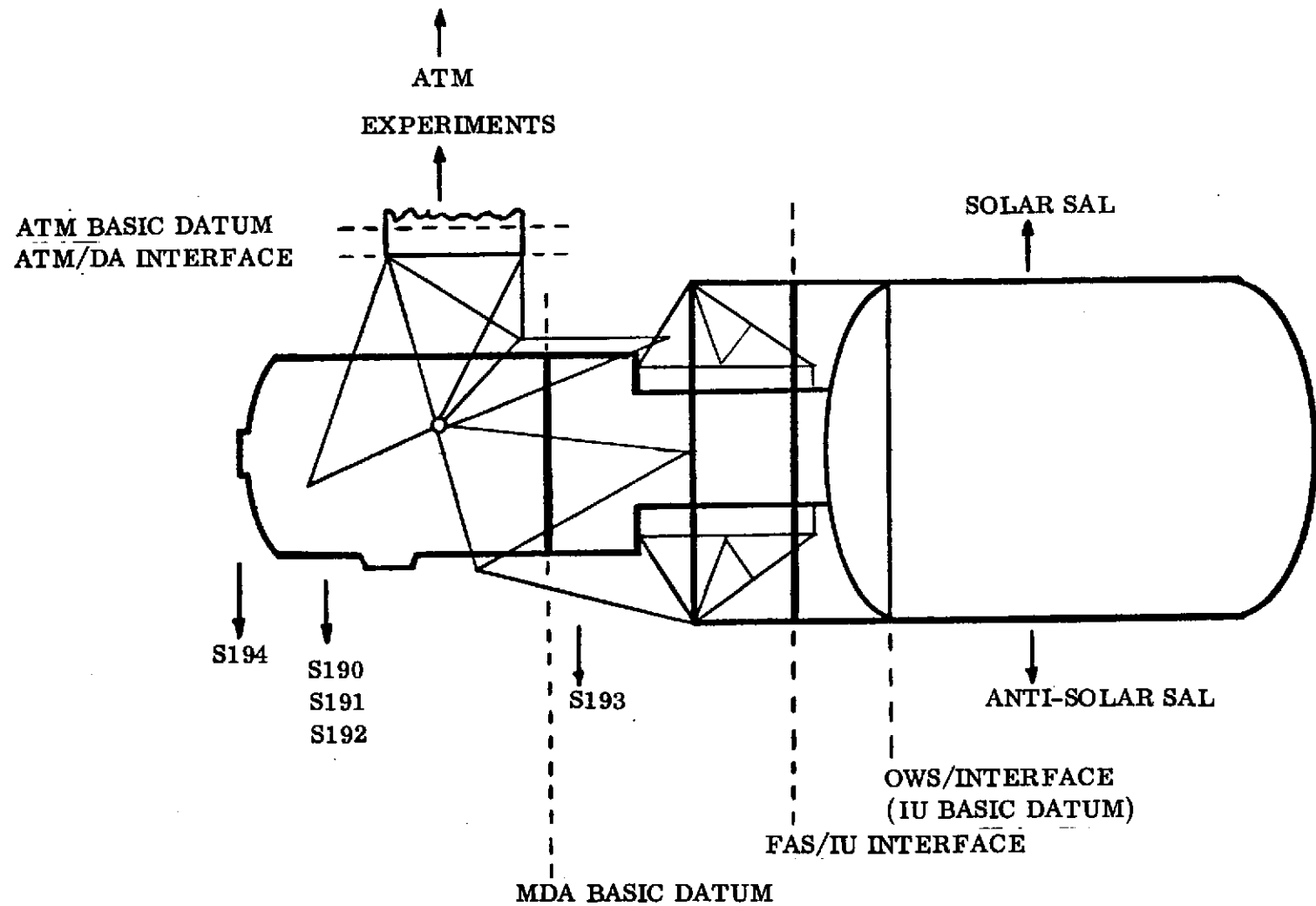
OWS/INTERFACE
(IU BASIC DATUM)

FAS/IU INTERFACE

MDA BASIC DATUM

Figure A-2. General configuration — reference locations.
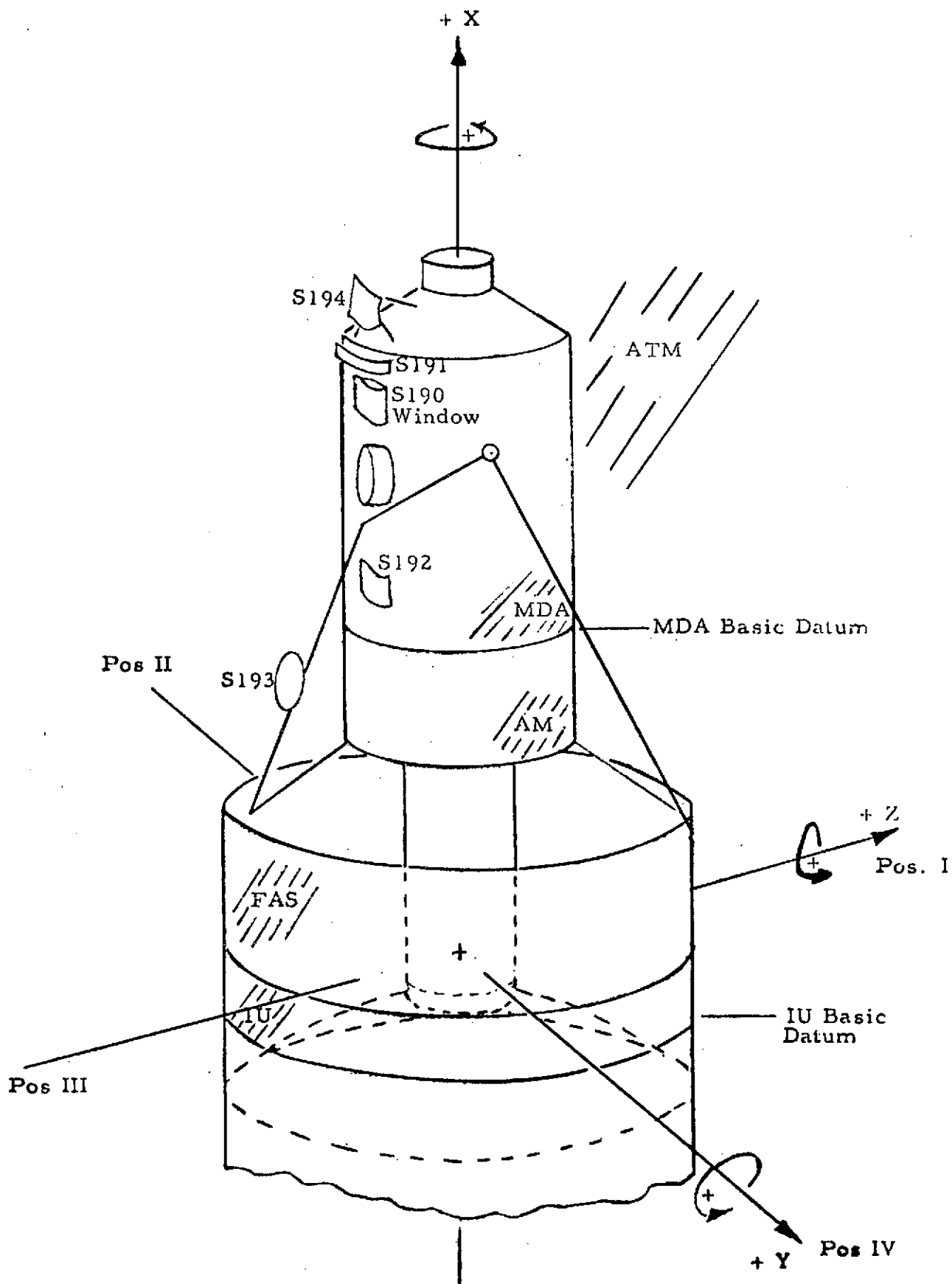
Figure A-3. General configuration — IU to MDA details.

TABLE A-1. ALIGNMENT ERROR COMPONENTS

MisAlignment Sources	Rotational Error Components About the Axes (Degree of Arc)						Remarks
	M_{vx}		M_{vy}		M_{vz}		
	Bias	Uncert	Bias	Uncert	Bias	Uncert	
STRUCTURAL							
ATM Experiment Optical Surface to ATM Basic Datum	0.0	±0.050	0.0	±0.050	0.0	±1.0	See Note △1
ATM Basic Datum to ATM/ Deployment Assembly (DA) Interface	0.0	±0.064	0.0	±0.037	0.0	±0.024	See Note △2
ATM/DA Interface to Fixed Airlock Shroud (FAS)/IU Interface	0.0	±0.250	0.0	±0.250	0.0	±0.049	See Note △3
FAS/IU Interface to OWS/IU Interface (IU Basic Datum)	0.0	±0.055	0.0	±0.050	0.0	±0.050	See Note △4
OWS/IU Interface to Solar [anti-solar] Scientific Airlock (SAL) Due to:							See Note △5
Waffle Pattern Location	-0.150 (+1.883)	±0.442	0.0	±0.0	0.0	±0.0	
Adapter Fitting Face	0.0	±0.500	0.0	±0.500	0.0	±0.0	
Assembly, Fitting to Wall	0.0	±0.0	0.0	±0.0	0.0	±0.500	
Wall Irregularity	0.0	±0.067	0.0	±0.067	0.0	±0.0	
Tank Cant	0.0	±0.0	0.0	±0.020	0.0	±0.020	
Tank Rotation	0.0	±0.047	0.0	±0.0	0.0	±0.0	
Pressure Effects	0.0	±0.0	0.027 [-0.027]	±0.0	0.0	±0.0	
FAS/IU Interface to MDA Basic Datum	0.0	±0.117	0.0	±0.047	0.0	±0.047	See Note △6

17

TABLE A-1. ALIGNMENT ERROR COMPONENTS (Concluded)

MisAlignment Sources	Rotational Error Components About the Axes (Degree of Arc)						Remarks
	M_{vx}		M_{vy}		M_{vz}		
	Bias	Uncert	Bias	Uncert	Bias	Uncert	
STRUCTURAL (Concluded)							
MDA Basic Datum to Axial Docking Port	0.0	±0.064	0.0	±0.096	0.0	±0.096	See Note △7
ST-124 Support Structure to Instrument Unit (IU) Basic Datum	0.0	±0.250	0.0	±0.250	0.0	±0.250	See Note △8
MDA Basic Datum to S190/MDA Interface	0.023	±0.037	0.038	±0.043	0.0	±0.020	See Note △9
MDA Basic Datum to S191/MDA Interface	-0.121	±0.051	-0.191	±0.115	0.0	±0.029	" " "
MDA Basic Datum to S192/MDA Interface	-0.017	±0.042	-0.057	±0.048	0.0	±0.045	" " "
MDA Basic Datum to S194/MDA Interface	-0.006	±0.040	0.059	±0.042	0.0	±0.029	
FAS/IU Interface to S193/MDA Interface	0.0	±0.102	0.0	±0.137	0.0	±0.057	See Note △10
MDA Axial Port to Docking Interface Calibration Scale	35	±0.083	0.0	±0.0	0.0	±0.0	See Note △11
THERMAL							
Solar Inertial Attitude	–	–	–	–	–	–	See Figure A-4 in Note △12
Z-LV ATTITUDE	–	–	–	–	–	–	See Note △12
DYNAMIC EFFECTS	–	–	–	–	–	–	See Note △13
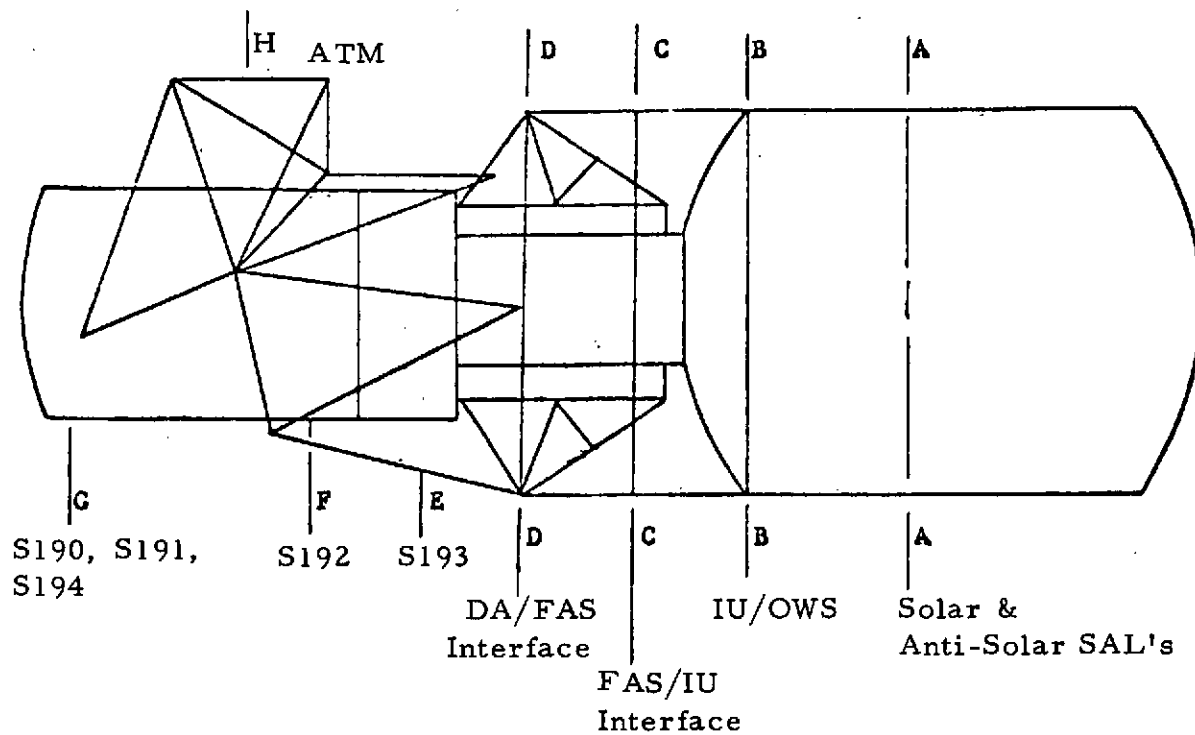
Figure A-4. Reference scheme for thermal deflections.

TABLE A-2. ROTATIONS RELATIVE TO PLANE A-A (deg)

	B-B	C-C	D-D	E	F	G	H
Hot Case	0.016	0.099	0.158	0.190	0.168	0.168	0.024
Cold Case	0.013	0.042	0.060	0.053	0.060	0.060	0.355
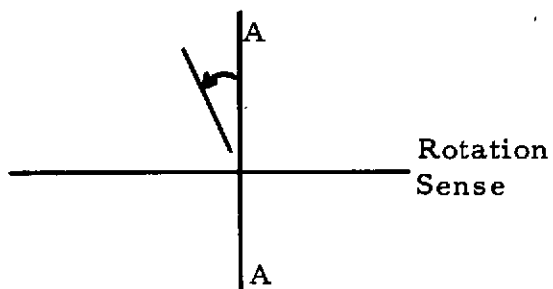
Note △₂   ATM BASIC DATUM TO ATM/DA INTERFACE

In the following sketch are the approximate dimensions [4] obtained for the ATM/DA attach points.
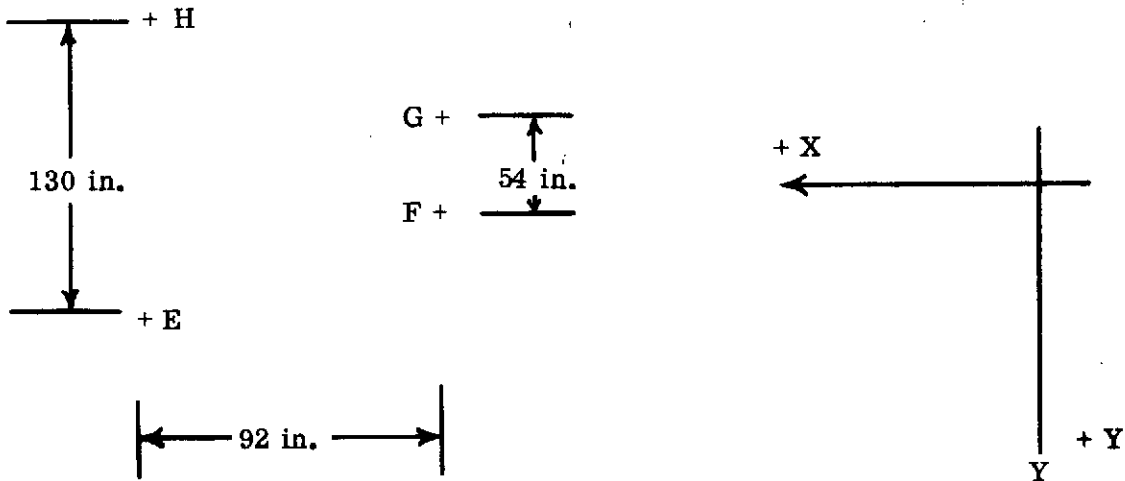
Tolerances on the locations of each attach point were assumed to be ±0.030 in. Therefore, the worst-case error about the Y-axis would occur as in the following sketch.
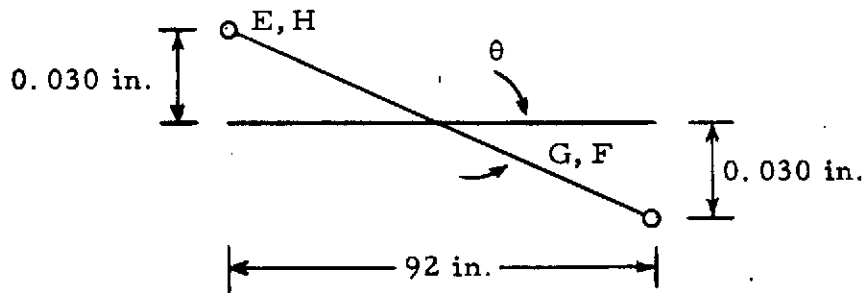
$$M_{VY} = \sin \theta \approx \theta = \frac{0.030 \text{ in.}}{46 \text{ in.}} \; (57.3 \text{ deg/rad}) = 0.037 \text{ deg},$$

$$M_{VY} = 0.0 \pm 0.037 \text{ deg.}$$

Similarly, worst-case misalignment about the X-axis would occur as in the following sketch.

20
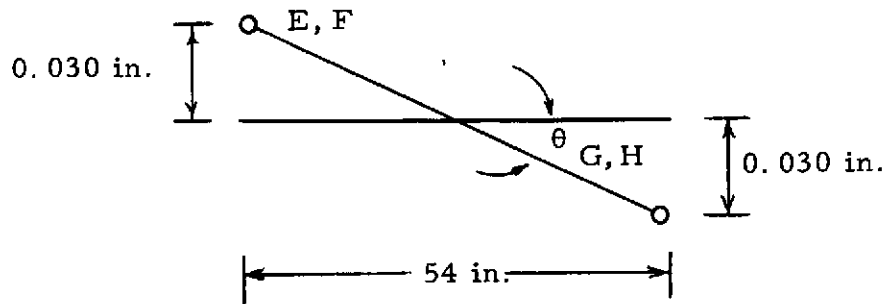
$$M_{VX} = \sin\theta \approx \theta = \frac{0.030 \text{ in.}}{27 \text{ in.}} \ (57.3 \text{ deg/rad}) = 0.064 \text{ deg,}$$

$$M_{VX} = 0.0 \pm 0.064 \text{ deg.}$$

For rotation about the Z-axis the worst case would occur when the attach points were all misaligned in the same direction as shown in the following sketch.
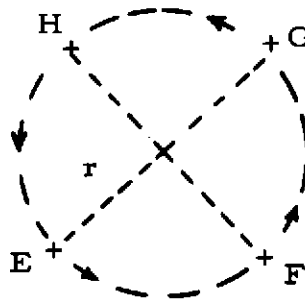
An effective radius (r) = 70.4 in. was calculated. Thus,

$$\frac{M_{VZ}}{2\pi} = \frac{0.030}{2\pi \ r} \quad ,$$

$$M_{VZ} = \frac{0.030 \text{ in.}}{70.4 \text{ in.}} \ (57.3 \text{ deg/rad}) = 0.024 \text{ deg,}$$

$$M_{VZ} = 0.0 \pm 0.024 \text{ deg.}$$

Note △3 ATM/DA INTERFACE TO FAS/IU INTERFACE

From References 4 and 5,

$$M_{VX} = M_{VY} \pm 0.250 \text{ deg.}$$

The rotational error about the Z-axis is calculated as in Note △2 except that the attach points can vary as much as 0.060 in. from nominal locations. Thus,

$$M_{VZ} = \frac{0.060 \text{ in.}}{70.4 \text{ in.}} \, (57.3 \text{ deg/rad}) = 0.049 \text{ deg,}$$

$$M_{VZ} = 0.0 \pm 0.049 \text{ deg.}$$

Note △4 IU BASIC DATUM TO FAS/IU INTERFACE

Position I in the interface plane is displaced a maximum of 0.125 in. circumferentially from Position I in the basic datum, [6,7], i.e.,

$$\frac{M_{VX}}{2\pi} = \frac{0.125}{\pi d} \quad, \quad \text{FAS/IU diameter (d)} = 260 \text{ in.,}$$

$$M_{VX} = \frac{2(0.125 \text{ in.})}{260 \text{ in.}} \, (57.3 \text{ deg/rad}) = 0.055 \text{ deg,}$$

$$M_{VX} = 0.0 \pm 0.055 \text{ deg.}$$

The interface plane is parallel to the basic datum to 0.226 in. [6,7]. Therefore, the maximum error would be
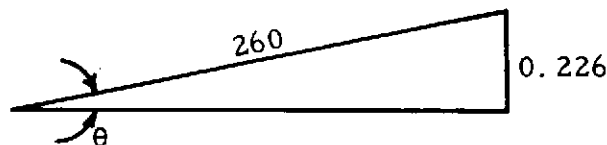
$$\sin \theta \approx \theta = \frac{0.226 \text{ in.}}{260 \text{ in.}} \ (57.3 \text{ deg/rad}) = 0.050 \text{ deg},$$

$$M_{VY} = M_{VZ} = 0.0 \pm 0.050 \text{ deg}.$$

Note ⑤ OWS/IU INTERFACE TO SOLAR [ANTI-SOLAR] SAL

A McDonnell Douglas letter[2] served as a basis for the alignments controlled by the OWS Alignment Control Drawing (ACD). The ACD, however, contains only the total misalignment tolerance for the SALs. Therefore, the component tolerances were used from the letter.

Note ⑥ FAS/IU INTERFACE TO MDA BASIC DATUM

Position I in the MDA datum is displaced a maximum of 0.125 in. circumferentially from Position I in the interface plane [5], i.e.,

$$\frac{M_{VX}}{2\pi} = \frac{0.125}{\pi \, d} \quad , \quad \text{MDA diameter (d)} = 121.6 \text{ in.},$$

$$M_{VX} = \frac{2 \, (0.125 \text{ in.})}{121.6 \text{ in.}} \ (57.3 \text{ deg/rad}) = 0.118 \text{ deg},$$

$$M_{VX} = 0.0 \pm 0.118 \text{ deg}.$$

The MDA datum is parallel to the interface plane to within 0.010 in. [5]. Thus, for maximum error,

2. McDonnell Douglas Astronautics Co., Western Division, Letter A3-850-KGOO-L-1590, Orbital Workshop (OWS) Alignment Tolerance to Support Scientific Airlock (SAL) Experiments, Huntington Beach, Calif., July 16, 1970.
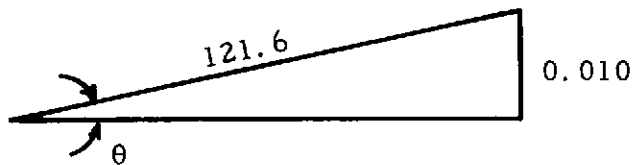
$$\sin \theta \approx \theta = M_{VY} + M_{VZ} = \frac{0.010 \text{ in.}}{121.6 \text{ in.}} \ (57.3 \text{ deg/rad}) = 0.047 \text{ deg,}$$

$$M_{VY} = M_{VZ} = 0.0 \pm 0.047 \text{ deg.}$$

Note ⚠ MDA BASIC DATUM TO AXIAL DOCKING PORT

Position I in the docking port plane is displaced a maximum of 0.020 in. circumferentially from Position I in the basic datum [8]. Thus,

$$\frac{M_{VX}}{2\pi} = \frac{0.020}{\pi d} \quad \text{docking port diameter (d)} = 35.92 \text{ in.,}$$

$$M_{VX} = \frac{2 \ (0.020 \text{ in.}) \ (57.3 \text{ deg/rad})}{35.92 \text{ in.}} = 0.064 \text{ deg,}$$

$$M_{VX} = 0.0 \pm 0.064 \text{ deg.}$$

The docking port plane is parallel to the basic datum to 0.060 in. [8]. For maximum error,
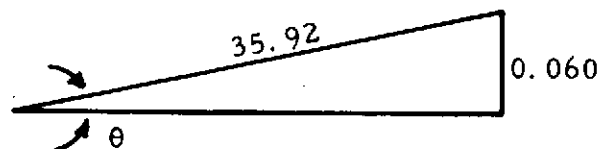
$$\sin \theta \approx \theta = M_{VY} = M_{VZ} = \frac{0.060 \text{ in.} (57.3 \text{ deg/rad})}{35.92 \text{ in.}} = 0.096 \text{ deg,}$$

$$M_{VY} = M_{VZ} = 0.0 \pm 0.096 \text{ deg.}$$

Note ⚠8 ST-124 SUPPORT STRUCTURE TO IU BASIC DATUM

From References 6 and 7, the X- and Z-axes of the support structure are perpendicular to a line between Positions II and IV to 0 deg, 15 min, i.e., $M_{VX} = M_{VZ} = 0.0 \pm 0.250$ deg. The Y- and Z-axes of the support structure are parallel to the IU basic datum to 0 deg, 15 min, i.e., $M_{VY} = 0.0 \pm 0.250$ deg.

Note ⚠9 MDA BASIC DATUM TO S190, S191, S192, S194/MDA INTERFACES

Measurements were made to each of four mounting pads for each experiment listed.[3] The differences in the measurements for any two of the pads were then converted to angular misalignments. The uncertainty associated with each angular misalignment was "1 to 2 min." Therefore, the misalignment error for one set of pads was assumed to be uniformly distributed between the measured misalignment minus 0 deg, 2 min, and the measured misalignment plus 0 deg, 2 min.

To obtain the misalignment error about the X-axis (M_{VX}), it was necessary to combine the angular misalignments for two sets of pads. It was therefore assumed that M_{VX} was uniformly distributed between the two measured angular misalignments. To obtain the total M_{VX}, the uncertainties in the previous paragraph were also considered. Thus, M_{VX} was assumed to be uniformly distributed between angular misalignment$_1$ minus 0 deg, 2 min, and angular misalignment$_2$ plus 0 deg, 2 min (angular misalignment$_1$ < angular misalignment$_2$).

---

3. W. E. Etherington, EREP Interface Measurements on the MDA Flight Article, Martin Marietta Corp., Denver, Col., Oct. 18, 1971; presented at Marshall Space Flight Center Oct. 20, 1971; attached to MSFC memorandum S&E-CSE-A-71-494, Oct. 26, 1971.

For example, for S190:

Angular misalignment between pads 1 and 2 = 1 min, 12 sec ± 2 min.

Angular misalignment between pads 3 and 4 = 1 min, 37 sec ± 2 min.

M_{VX} is uniformly distributed between (0 deg, 1 min, 12 sec – 0 deg, 2 min) and (0 deg, 1 min, 37 sec + 0 deg, 2 min), or

$$M_{VX} = 0 \text{ deg, } 1 \text{ min, } 24.5 \text{ sec } \pm 0 \text{ deg, } 2 \text{ min, } 12.5 \text{ sec}$$

$$= 0.023 \text{ deg } \pm 0.037 \text{ min.}$$

M_{VX} and M_{VY} were determined for S190, S191, S192, and S194 using the above method.

The tolerance on the location center of each mounting hole is ± 0.007 in. [9]. Assuming all hole errors are in the same direction because of the use of a master tool of some type and choosing an effective radius of 20 in.,

$$M_{VZ} = \frac{0.007 \text{ in.}}{20 \text{ in.}} \ (57.3 \text{ deg/rad}) = 0.020 \text{ deg,}$$

$$M_{VZ} = 0.0 \pm 0.020 \text{ deg.}$$

M_{VZ} for S191, S192, and S194 was similarly derived, i.e., using tolerances on bolt hole locations and choosing a radius for conversion to rotational error.

Note ⚠️10 FAS/IU INTERFACE TO S193/DA INTERFACE

The rotational uncertainty of the interface plane about the Y-axis is ± 0 deg, 7 min = ± 0.125 deg [10].

In addition, the mounting pads must be parallel to the interface plane to ± 0.005 in. [10]. Assuming the mounting pads are misaligned in the worst

case condition, using a distance of 23.65 in. between the appropriate pads and adding the resulting misalignment directly to the aforementioned ± 0.125 deg, then

$$M_{VY} = 0.125 \text{ deg} + \left[\frac{0.005 \text{ in.}}{23.65 \text{ in.}} \left(57.3 \text{ deg/rad} \right) \right]$$

$$= 0.125 \text{ deg} + 0.012 \text{ deg} = 0.137 \text{ deg,}$$

$$M_{VY} = 0.0 \pm 0.137 \text{ deg.}$$

The error about the X-axis from the misalignment of the interface plane assuming misalignment in the worst-case condition and using a distance of 63.37 in. is

$$M_{VX} = \frac{0.10 \text{ in.}}{63.37 \text{ in.}} \left(57.3 \text{ deg/rad} \right) = 0.090 \text{ deg.}$$

Again adding the misalignment of the pads to the interface plane,

$$M_{VX} = 0.0 \pm 0.102 \text{ deg.}$$

Misalignment about the Z-axis was determined as in Note ⚠9 , assuming an effective radius of 30 in. and a bolt hole tolerance of ± 0.030 in.

$$M_{VZ} = \frac{0.030 \text{ in.}}{30 \text{ in.}} \left(57.3 \text{ deg/rad} \right) = 0.057 \text{ deg,}$$

$$M_{VZ} = 0.0 \pm 0.057 \text{ deg.}$$

Note ⚠11   MDA AXIAL PORT TO DOCKING INTERFACE CALIBRATION SCALE

The interface calibration scale is located as follows [11] ,
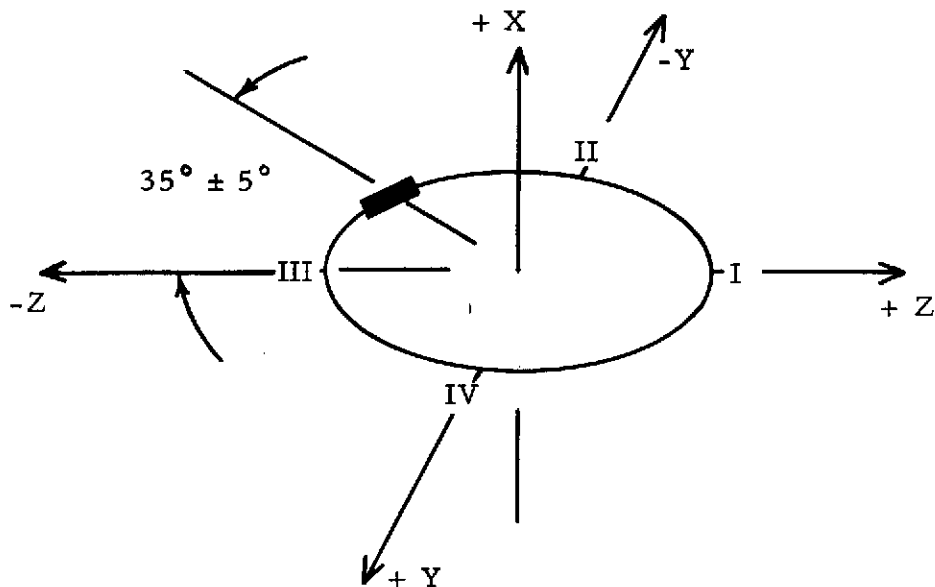
which yields a misalignment of 35 deg ± 0.083 deg about the X-axis (M_{VX}).

$$M_{VY} = M_{VZ} = 0 .$$

Note ⚠️12 THERMAL

In Reference 1, thermal bending misalignments between various cluster locations were calculated. Misalignments were calculated for both the hot and cold thermal extreme cases. The thermal bending misalignment was assumed to have a uniform frequency distribution between the extreme cases. The mean of the resulting uniform distribution was treated as a bias error and the distance to the end points as the uncertainty. The thermal numbers in this report were calculated for the solar inertial attitude mode. Thus, it was assumed that thermal bending would occur about the Y-axis only. See Figure A-4 for the thermal bending predictions [1].

For thermal bending misalignments in the Z-LV (E) attitude, an in-house (ASTN) study was performed, which was concerned only with the DA trusses. Thus, the same misalignments were used for all cases in Z-LV that involved locations on "opposite sides" of the DA. The in-house study examined

a number of Z-LV cases, varying such parameters as beta angle and the time in the orbit. From all data, temperatures were chosen for the individual truss members such that the worst-case thermal bending misalignments were obtained. The misalignments are as follows:

$$M_{VX} = \pm 0.450 \text{ deg,}$$

$$M_{VY} = \pm 0.384 \text{ deg,}$$

$$M_{VZ} = \pm 0.166 \text{ deg .}$$

Note $\triangle{13}$ DYNAMIC EFFECTS

The misalignment caused by dynamic effects was determined to be negligible due to the small magnitudes. (Refer to Reference 1 and footnote 1.)

APPENDIX B

SKYLAB MISALIGNMENT PREDICTIONS

This appendix describes the method of combining the alignment error components to obtain the total predicted misalignments. The example case concerns the misalignment of the ATM Basic Datum and the Anti-Solar Scientific Airlock (SAL) in rotation about the Y-cluster axis for the solar inertial attitude.

The following procedure was used to obtain the total predicted misalignment:

1. The bias errors were added directly to obtain the bias error for the total misalignments.

2. The uncertainties were treated as uniform distributions with zero means. A random sampling technique was employed to obtain the total uncertainty error.

3. The total misalignment prediction for any case is then the total bias error plus or minus the total uncertainty error.

Figure B-1 shows the Skylab reference locations. The example case misalignment components (from Appendix A) are listed in Table B-1. Figure B-2 is an example of the input data for the misalignment program, and Figure B-3 is a listing of the misalignment program. Figures B-4 and B-5 show the program output and the resulting frequency distribution plot, respectively. Figures B-6 and B-7 show other program outputs and the resulting cumulative probability plot, respectively. Total misalignment predictions are listed in Table B-2.

ATM
EXPERIMENTS

ATM BASIC DATUM
ATM/DA INTERFACE

SOLAR SAL

S194

S190
S191
S192

POS II   +Z
-Y   POS I

+X   -X

+Y

-Z   POS IV
POS III

S193

ANTI-SOLAR SAL

OWS/IU INTERFACE
(IU BASIC DATUM)

MDA
BASIC DATUM
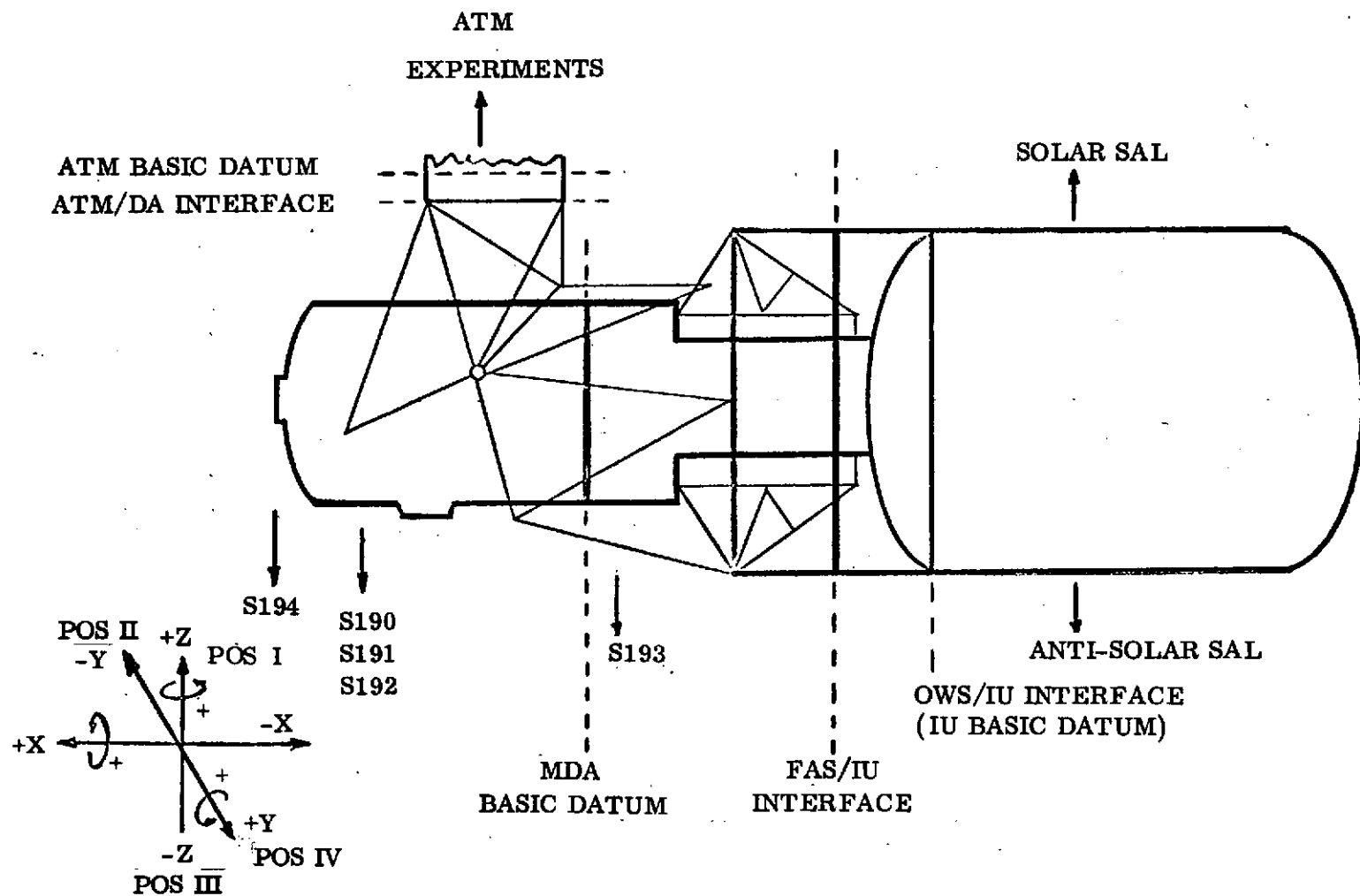
FAS/IU
INTERFACE

Figure B-1. General configuration.

TABLE B-1. EXAMPLE CASE ALIGNMENT ERROR COMPONENTS

Misalignment Sources	E_Y - Degree of Arc in Rotation about the Y-Axis
Structural	
ATM Basic Datum to ATM/DA Interface	± 0.037
ATM/DA Interface to FAS/IU Interface	± 0.250
FAS/IU Interface to OWS/IU Interface	± 0.050
OWS/IU Interface to Anti-Solar SAL	
Adapter Fitting Face	± 0.500
Wall Irregularity	± 0.067
Tank Cant	± 0.020
Pressure Effects	-0.027
Thermal	
ATM Basic Datum to Anti-Solar SAL	-0.190 ± 0.166

```
12453
 7
                    0.037        0.0
                    0.250        0.0
                    0.050        0.0
                    0.500        0.0
                    0.067        0.0
                    0.020        0.0
                    0.166        0.0
0.015
20 000
```

Where   12453 is the Random Number Seed.

7 is the number of component distributions.

0.037, 0.250, 0.050, etc., represent the maximum deviations from the mean for the component distributions.

0.0, 0.0, etc., represent the means of the component distributions.

0.015 is the cell width or the increment used to group total misalignments to form the frequency distribution.

20 000 is the number of simulations.

Figure B-2. Example case input data.

```
RUN,//T ALINEX,442068,HOVERKBIN207,3,150    . ** MISALIGNMENT ERROR ANALYSIS**
FOR,IS MAIN
      DIMENSION RANGE(99),XMEAN(99),NCNT(500),NCNTP(300)
      INTEGER R,W
C   NCNT(I) IS THE NUMBER OF HITS IN INCREMENT(I)
C   IX IS THE RANDOM NUMBER STARTER
      R=5
      W=6
      READ (R,101) IX
  101 FORMAT (I5)
C   NDIST IS THE NUMBER OF INDIVIDUAL DISTRIBUTIONS
   99 WRITE (W,98)
   98 FORMAT (1H1)
      READ (R,106) NDIST
  106 FORMAT (I2)
      IF (NDIST) 200,200,90
   90 UPLIM=0.
      BLIMT=0.
C   DATA INPUT LOOP
      DO 111 I=1,NDIST
C   RANGE(I) IS THE MAGNITUDE OF THE MAXIMUM DEVIATION ABOUT THE MEAN
C      OF DISTRIBUTION(I)
C   XMEAN(I) IS THE MEAN OF DISTRIBUTION(I)
      READ (R,105) RANGE(I),XMEAN(I)
  105 FORMAT (10X,2F10.4)
C   UP IS THE MAXIMUM POSITIVE ERROR
      UPLIM=UPLIM+XMEAN(I)+RANGE(I)
C   BLIMT IS THE MAXIMUM NEGATIVE ERROR
      BLIMT=BLIMT+XMEAN(I)-RANGE(I)
  111 CONTINUE
C   STEP IS THE ERROR INCREMENT SIZE
      READ (R,104) STEP
  104 FORMAT (F10.4)
      DUM1=ABS(BLIMT/STEP)
      IDUM=IFIX(DUM1)
      DUM2=FLOAT(IDUM)
      IF (DUM1-DUM2) 102,107,102
  102 IDUM=IDUM+1
  107 BLIMT=STEP*FLOAT(IDUM)*(BLIMT/ABS(BLIMT))
C   NSAMS IS THE NUMBER OF SAMPLES DESIRED
      READ (R,131)NSAMS
  131 FORMAT (I6)
C   INCS IS THE TOTAL NUMBER OF INCREMENTS AND MUST BE LESS THAN 500
      INCS=1+IFIX((UPLIM-BLIMT)/STEP)
      DO 140 I=1,INCS
  140 NCNT(I)=0
      TMEAN=0.
C   THIS LOOP RUNS THE SAMPLES
      DO 160 J=1,NSAMS
C   TOTER IS THE TOTAL ERROR FOR ONE SAMPLING
      TOTER=0.
C   THIS LOOP CALCULATES ONE SAMPLE
      DO 150 I=1,NDIST
      IY=IX*316231
      IF (IY) 145,146,146
  145 IY=IY+34359738367
  146 YFL=IY
      YFL=YFL/343597384.E2
      IX=IY
C   RNDER IS RANDOM ERROR FOR ONE DISTRIBUTION
      RNDER=(XMEAN(I)-RANGE(I))+2.*YFL*RANGE(I)
```

Figure B-3. Misalignment program listing.

```
          TOTER=TOTER+RNDER
      150 CONTINUE
          IF (TOTER-BLIMT) 200,155,153
      153 IF (TOTER-UPLIM) 155,155,200
C     INDEX IS THE INDEX OF THE INCREMENT CONTAINING TOTER
      155 INDEX=1+ IFIX((TOTER-BLIMT)/STEP)
          NCNT(INDEX)=NCNT(INDEX)+1
          TMEAN = TMEAN + TOTER
      160 CONTINUE
C     TMEAN IS THE MEAN OF THE TOTAL ERRORS
          TMEAN = TMEAN/FLOAT(NSAMS)
C     SIGMA IS THE STANDARD DEVIATION
          SIGMA=0.
C     THIS LOOP CALCULATES THE SMALLEST ERROR  OF EACH INCREMENT AND SUMS
C     THE SQUARES OF THE DELTAS
          DO 905 I=1,INCS
C     ERRLO IS THE LOWEST ERROR OF A SINGLE INCREMENT
          ERRLO=BLIMT+STEP*FLOAT(I-1)
C ERRHI IS THE HIGHEST ERROR OF A SINGLE INCREMENT
          ERRHI=ERRLO+ STEP
          WRITE (W,50) ERRLO,ERRHI,NCNT(I)
      50 FORMAT  (1H ,2F10.4,I10)
C     HSTEP IS HALF STEP
          HSTEP=(STEP/2.)-TMEAN
C     THIS IS THE SUM OF THE SQUARES FOR THE STANDARD DEVIATION CALCULATION
          SIGMA=((ERRLO+HSTEP)**2)*NCNT(I)+SIGMA
      905 CONTINUE
          WRITE (W,98)
C     IDUM IS CURRENTLY THE INDEX OF THE INCREMENT ON THE NEGATIVE SIDE OF ZERO
          IF (INCS-2*IDUM) 167,167,168
C     ICNT IS THE NUMBER OF MAGNITUDES OF ERROR INCREMENTS
      167 ICNT=IDUM
          G T  169
      168 ICNT=INCS-IDU
      169 CONTINUE
          DO 170 I=1,INCS
C     NCNTP(I) IS THE NUMBER ERROR FOR INCREMENT MAGNITUDE(I)
      170 NCNTP(I)=0
C     FROM HERE TO 180 CALCULATES HITS PER MAGNITUDE INCREMENT
          DO 175 I=1,IDUM
C     IDUM1 IS THE INDEX OF THE MAGNITUDE LESS THAN ZERO
          IDUM1=IDUM-I+1
      175 NCNTP(I)=NCNT(IDUM1)
C     II IS THE NUMBER OF POSITIVE INCREMENTS
          II=INCS-IDUM
          DO 180 I=1,II
C     IDUM1 IS THE INDEX OF THE COUNT FOR POSITIVE ERRORS
          IDUM1=IDUM+I
      180 NCNTP(I)=NCNTP(I)+NCNT(IDUM1)
C     ICNTS IS THE ACCUMULATED NUMBER OF HITS
          ICNTS=0
C     THIS LOOP CALCULATES ERROR INCREMENTS, TOTALS, AND ACCUMULATIVE PROBABILITY
          DO 190 I=1,ICNT
C     BEROR IS THE SMALLEST ERROR  IN  A MAGNITUDE INCREMENT
          BEROR=STEP*FLOAT(I-1)
C     HEROR IS THE LARGEST ERROR IN A MAGNITUDE INCREMENT
          HEROR=STEP*FLOAT(I)
          ICNTS=ICNTS+NCNTP(I)
C     ACPRB IS THE ACCUMULATIVE PROBABILITY
          ACPRB=FLOAT(ICNTS)/FLOAT(NSAMS)
      190 WRITE (W,920) BEROR,HEROR,NCNTP(I),ACPRB,ICNTS
```

Figure B-3. Misalignment program listing (continued).

```
  920 FORMAT (1H ,2F10.4,I5,F10.4,I6)
C  THIS IS THE SQUARE ROOT OF THE SUM OF SQUARES OF DELTAS DIVIDED BY
C    NUMBER OF SAMPLES
     SIGMA=SQRT(SIGMA/NSAMS)
     WRITE (W,930) TMEAN,SIGMA
  930 FORMAT (1H0,12HTHE MEAN IS ,F10.4/1H ,26HTHE STANDARD DEVIATION IS
    1 ,F10.4)
     WRIT  (W,910) NSAMS
  910 FORMAT (1H ,10HTHERE WERE,I6,8H SAMPLES)
     GO TO 99
  200 CONTINUE

     STOP
     END
MAP,IX A,B
LIB SYS$*MSFC$.
XQT R
```

Figure B-3. Misalignment program listing (concluded).

Misalignment Range		No. of Samples in Range	Misalignment Range		No. of Samples in Range	Misalignment Range		No. of Samples in Range
-1.0950	-1.0800	0	-.2700	-.2550	267	.5700	.5850	103
-1.0800	-1.0650	0	-.2550	-.2400	277	.5850	.6000	93
-1.0650	-1.0500	0	-.2400	-.2250	258	.6000	.6150	83
-1.0500	-1.0350	0	-.2250	-.2100	265	.6150	.6300	53
-1.0350	-1.0200	0	-.2100	-.1950	289	.6300	.6450	76
-1.0200	-1.0050	0	-.1950	-.1800	260	.6450	.6600	70
-1.0050	-.9900	0	-.1800	-.1650	286	.6600	.6750	65
-.9900	-.9750	0	-.1650	-.1500	261	.6750	.6900	56
-.9750	-.9600	0	-.1500	-.1350	292	.6900	.7050	46
-.9600	-.9450	0	-.1350	-.1200	302	.7050	.7200	41
-.9450	-.9300	1	-.1200	-.1050	312	.7200	.7350	36
-.9300	-.9150	3	-.1050	-.0900	296	.7350	.7500	32
-.9150	-.9000	2	-.0900	-.0750	337	.7500	.7650	24
-.9000	-.8850	3	-.0750	-.0600	316	.7650	.7800	28
-.8850	-.8700	4	-.0600	-.0450	297	.7800	.7950	17
-.8700	-.8550	3	-.0450	-.0300	299	.7950	.8100	13
-.8550	-.8400	5	-.0300	-.0150	292	.8100	.8250	8
-.8400	-.8250	9	-.0150	-.0000	293	.8250	.8400	7
-.8250	-.8100	15	.0000	.0150	276	.8400	.8550	8
-.8100	-.7950	17	.0150	.0300	314	.8550	.8700	7
-.7950	-.7800	12	.0300	.0450	282	.8700	.8850	3
-.7800	-.7650	17	.0450	.0600	305	.8850	.9000	2
-.7650	-.7500	24	.0600	.0750	293	.9000	.9150	2
-.7500	-.7350	28	.0750	.0900	295	.9150	.9300	0
-.7350	-.7200	34	.0900	.1050	283	.9300	.9450	9
-.7200	-.7050	31	.1050	.1200	297	.9450	.9600	3
-.7050	-.6900	44	.1200	.1350	304	.9600	.9750	1
-.6900	-.6750	49	.1350	.1500	325	.9750	.9900	3
-.6750	-.6600	64	.1500	.1650	276	.9900	1.0050	
-.6600	-.6450	49	.1650	.1800	326	1.0050	1.0200	3
-.6450	-.6300	55	.1800	.1950	311	1.0200	1.0350	
-.6300	-.6150	72	.1950	.2100	318	1.0350	1.0500	
-.6150	-.6000	87	.2100	.2250	294	1.0500	1.0650	
-.6000	-.5850	110	.2250	.2400	285	1.0650	1.0800	2
-.5850	-.5700	134	.2400	.2550	252	1.0800	1.0950	0
-.5700	-.5550	137	.2550	.2700	284			
-.5550	-.5400	116	.2700	.2850	258			
-.5400	-.5250	121	.2850	.3000	243			
-.5250	-.5100	150	.3000	.3150	254			
-.5100	-.4950	129	.3150	.3300	265			
-.4950	-.4800	172	.3300	.3450	239			
-.4800	-.4650	174	.3450	.3600	248			
-.4650	-.4500	173	.3600	.3750	236			
-.4500	-.4350	201	.3750	.3900	223			
-.4350	-.4200	209	.3900	.4050	198			
-.4200	-.4050	198	.4050	.4200	186			
-.4050	-.3900	234	.4200	.4350	232			
-.3900	-.3750	214	.4350	.4500	186			
-.3750	-.3600	226	.4500	.4650	171			
-.3600	-.3450	229	.4650	.4800	162			
-.3450	-.3300	221	.4800	.4950	153			
-.3300	-.3150	237	.4950	.5100	163			
-.3150	-.3000	256	.5100	.5250	149			
-.3000	-.2850	264	.5250	.5400	129			
-.2850	-.2700	254	.5400	.5550	125			
			.5550	.5700	121			

Figure B-4.   Example case program output.

Frequency of M_{vy}
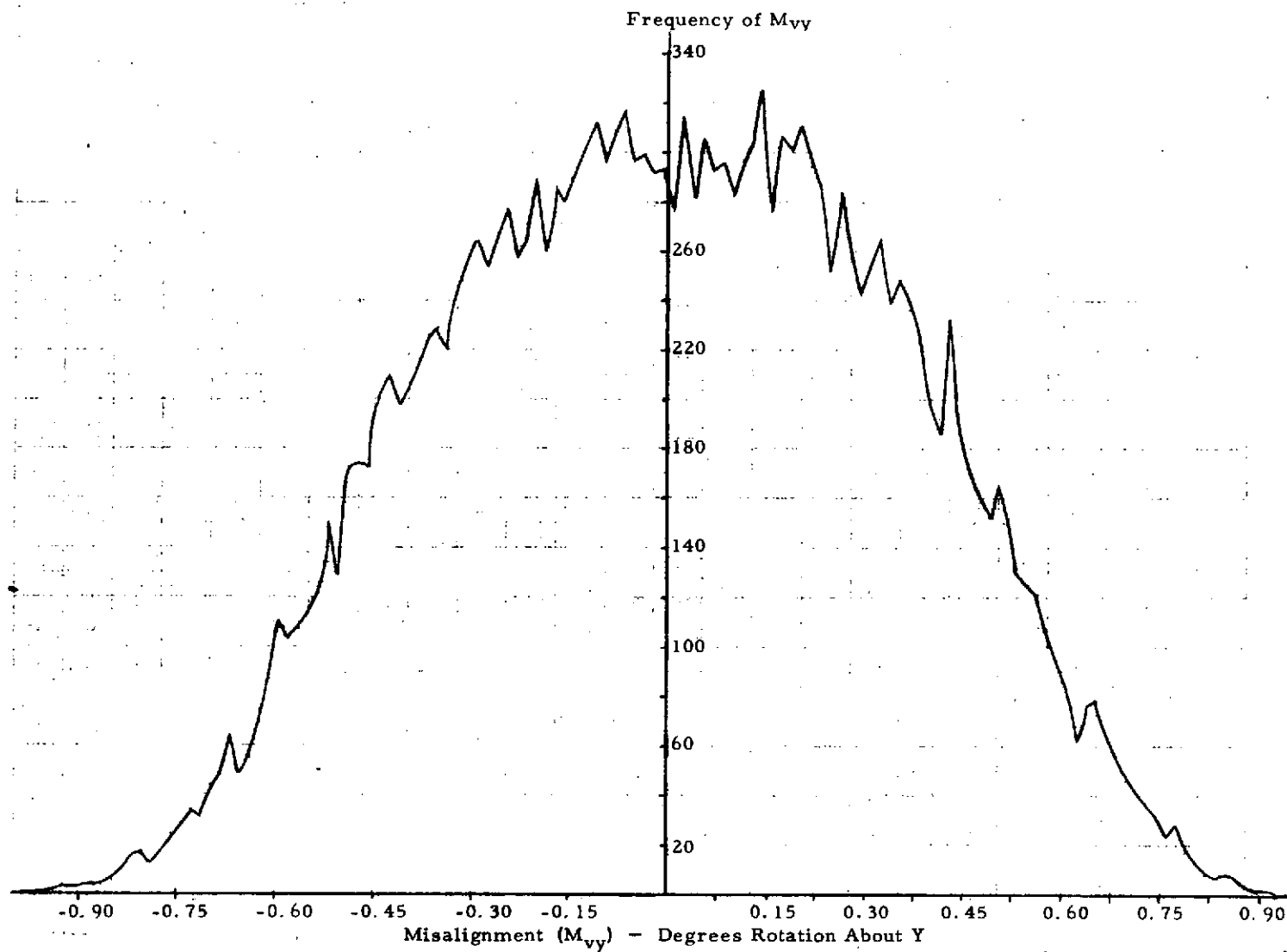

Misalignment (M_{vy}) — Degrees Rotation About Y

Figure B-5. Frequency distribution of total misalignment.

Misalignment Range		No. of Samples in Range	Cumulative		Misalignment Range		No. of Samples in Range	Cumulative	
			% of Samples	No. of Samples				% of Samples	No. of Samples
.0000	.0150	569	.0284	569					
.0150	.0300	606	.0587	1175	.8250	.8400	16	.9978	19956
.0300	.0450	581	.0878	1756	.8400	.8550	13	.9984	19969
.0450	.0600	602	.1179	2358	.8550	.8700	10	.9989	19979
.0600	.0750	609	.1483	2967	.8700	.8850	7	.9993	19986
.0750	.0900	604	.1785	3571	.8850	.9000	5	.9995	19991
.0900	.1050	579	.2075	4150	.9000	.9150	4	.9997	19995
.1050	.1200	609	.2379	4759	.9150	.9300	3	.9999	19998
.1200	.1350	606	.2682	5365	.9300	.9450	1	.9999	19999
.1350	.1500	617	.2991	5982	.9450	.9600	0	.9999	19999
.1500	.1650	557	.3269	6539	.9600	.9750	1	1.0000	20000
.1650	.1800	592	.3565	7131	.9750	.9900	0	1.0000	20000
.1800	.1950	561	.3846	7692	.9900	1.0050	0	1.0000	20000
.1950	.2100	599	.4145	8291	1.0050	1.0200	0	1.0000	20000
.2100	.2250	559	.4425	8850	1.0200	1.0350	0	1.0000	20000
.2250	.2400	543	.4696	9393	1.0350	1.0500	0	1.0000	20000
.2400	.2550	529	.4961	9922	1.0500	1.0650	0	1.0000	20000
.2550	.2700	551	.5236	10473	1.0650	1.0800	0	1.0000	20000
.2700	.2850	512	.5492	10985	1.0800	1.0950	0	1.0000	20000
.2850	.3000	507	.5746	11492					
.3000	.3150	510	.6001	12002					
.3150	.3300	502	.6252	12504					
.3300	.3450	460	.6482	12964					
.3450	.3600	477	.6720	13441					
.3600	.3750	462	.6951	13903					
.3750	.3900	437	.7170	14340					
.3900	.4050	402	.7371	14742					
.4050	.4200	384	.7563	15126					
.4200	.4350	441	.7783	15567					
.4350	.4500	387	.7977	15954					
.4500	.4650	344	.8149	16298					
.4650	.4800	336	.8317	16634					
.4800	.4950	325	.8479	16959					
.4950	.5100	292	.8625	17251					
.5100	.5250	299	.8775	17550					
.5250	.5400	250	.8900	17800					
.5400	.5550	241	.9020	18041					
.5550	.5700	228	.9134	18269					
.5700	.5850	204	.9236	18473					
.5850	.6000	203	.9338	18676					
.6000	.6150	170	.9423	18846					
.6150	.6300	135	.9490	18981					
.6300	.6450	131	.9554	19112					
.6450	.6600	127	.9619	19239					
.6600	.6750	129	.9684	19368					
.6750	.6900	105	.9736	19473					
.6900	.7050	90	.9781	19563					
.7050	.7200	72	.9817	19635					
.7200	.7350	70	.9852	19705					
.7350	.7500	60	.9882	19765					
.7500	.7650	48	.9906	19813					
.7650	.7800	45	.9929	19858					
.7800	.7950	29	.9943	19887					
.7950	.8100	30	.9958	19917					
.8100	.8250	23	.9970	19940					

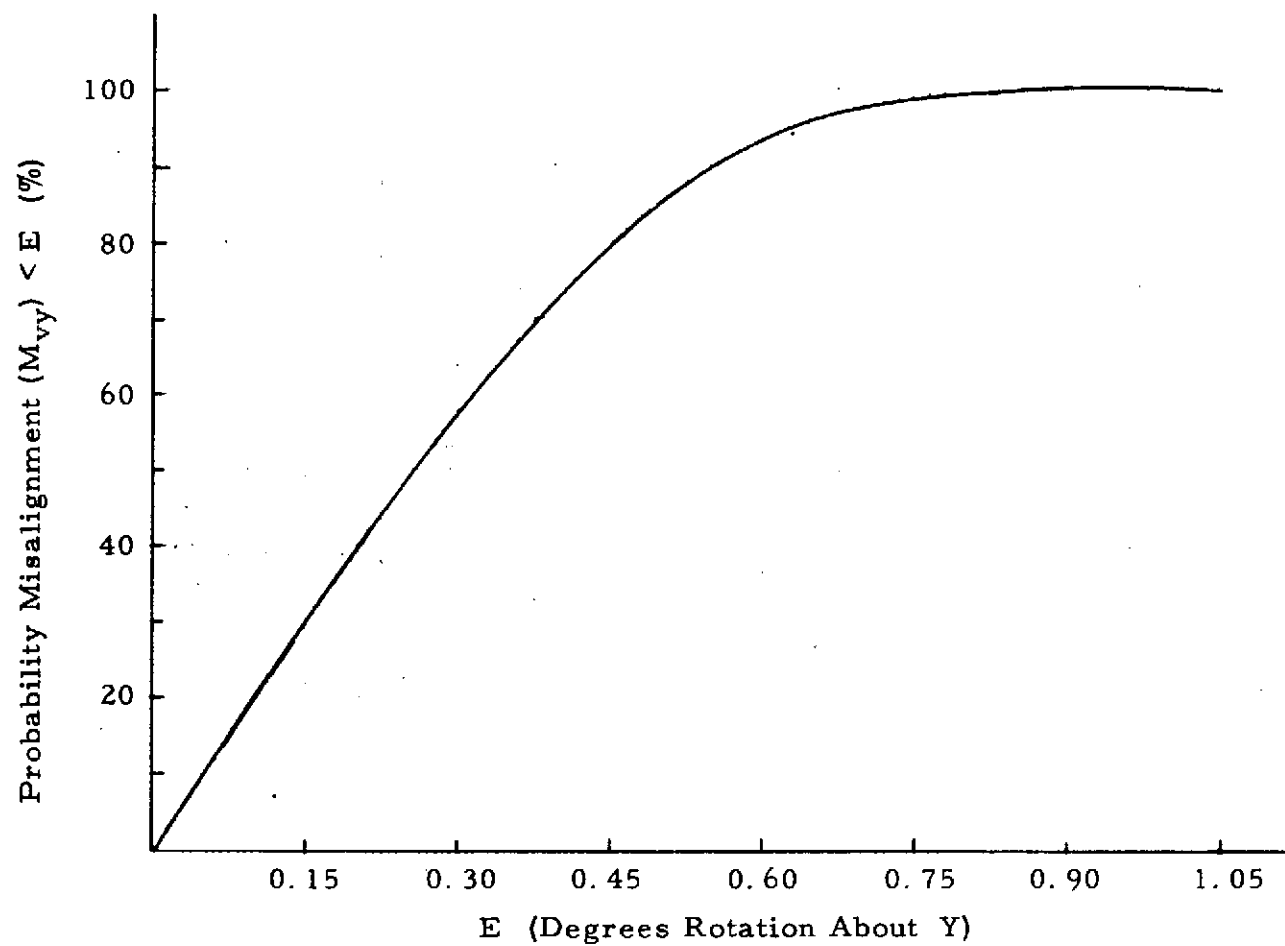Figure B-6.   Example case program output.

Figure B-7. Cumulative probability plot for total misalignment.

TABLE B-2. TOTAL MISALIGNMENT PREDICTIONS

Case	Total Rotational Misalignment About the Specified Axis (Degrees of Arc)						Remarks
	M_{vx}		M_{vy}		M_{vz}		
	Bias	Uncert.	Bias	Uncert.	Bias	Uncert.	
Solar Scientific Airlock (SAL) to ATM Basic Datum (Solar Inertial Attitude)	-0.150	±1.065	-0.163	±0.825	0.0	±0.559	General: The uncertainties are associated with a probability of 99.7%.
Anti-Solar SAL to ATM Basic Datum (Solar Inertial Attitude)	1.883	±1.065	-0.217	±0.825	0.0	±0.559	
Anti-Solar SAL to ATM Basic Datum (Z-LV Attitude)	1.883	±1.305	-0.027	±1.005	0.0	±0.810	
Solar SAL to Anti-Solar SAL (Solar Inertial Attitude)	2.033	±1.500	0.054	±0.982	0.0	±0.950	
ATM Basic Datum to S190/MDA Interface (Z-LV Attitude)	0.023	±0.727	0.038	±0.630	0.0	±0.242	
ATM Basic Datum to S190/MDA Interface (Solar Inertial Attitude)	0.023	±0.386	-0.038	±0.475	0.0	±0.110	

TABLE B-2. TOTAL MISALIGNMENT PREDICTIONS (Continued)

Case	Total Rotational Misalignment About the Specified Axis (Degrees of Arc)						Remarks
	M_{vx}		M_{vy}		M_{vz}		
	Bias	Uncert	Bias	Uncert	Bias	Uncert	
ATM Basic Datum to S191/MDA Interface (Z-LV Attitude)	-0.121	±0.736	-0.191	±0.676	0.0	±0.248	
ATM Basic Datum to S191/MDA Interface (Solar Inertial Attitude)	-0.121	±0.400	-0.267	±0.524	0.0	±0.118	
ATM Basic Datum to S192/MDA Interface (Z-LV Attitude)	-0.017	±0.737	-0.057	±0.628	0.0	±0.254	
ATM Basic Datum to S192/MDA Interface (Solar Inertial Attitude)	-0.017	±0.390	-0.133	±0.480	0.0	±0.132	
ATM Basic Datum to S193/DA Interface (Z-LV Attitude)	0.0	±0.759	0.0	±0.688	0.0	±0.267	
ATM Basic Datum to S193/DA Interface (Solar Inertial Attitude)	0.0	±0.429	-0.068	±0.548	0.0	±0.140	
ATM Basic Datum to S194/MDA Interface (Z-LV Attitude)	-0.006	±0.742	0.059	±0.625	0.0	±0.250	
ATM Basic Datum to S194/MDA Interface (Solar Inertial Attitude)	-0.006	±0.390	-0.017	±0.476	0.0	±0.118	
Anti-Solar SAL to S190/MDA Interface (Solar Inertial Attitude)	1.903	±0.969	-0.103	±0.608	0.0	±0.561	
ATM Basic Datum to MDA Docking Interface Calibration Scale	35	±0.435	-0.076	±0.510	0.0	±0.355	
ST-124 to S190/MDA Interface	+0.023	±0.355	+0.128	±0.316	0.0	±0.305	
ST-124 to S191/MDA Interface	-0.121	±0.360	-0.101	±0.360	0.0	±0.310	
ST-124 to S192/MDA Interface	-0.017	±0.357	+0.033	±0.318	0.0	±0.313	
ST-124 to S193/DA Interface	0.0	±0.340	+0.097	±0.370	0.0	±0.315	
ST-124 to S194/MDA Interface	-0.006	±0.357	+0.149	±0.317	0.0	±0.308	

TABLE B-2. TOTAL MISALIGNMENT PREDICTIONS (Concluded)

| Case | Total Rotational Misalignment About the Specified Axis. (Degrees of Arc) | | | | | | Remarks |
| | M_{vx} | | M_{vy} | | M_{vz} | | |
	Bias	Uncert	Bias	Uncert	Bias	Uncert	
MDA DOCKING INTERFACE CALIBRATION SCALE TO:							
S190A/MDA Interface	0.023	±0.160	0.038	±0.135	0.0	±0.114	
S190B/OWS Interface	1.994	±1.005	-0.141	±0.640	0.114	±0.620	
S191/MDA Interface	-0.121	±0.170	-0.191	±0.205	0.0	±0.120	
S192/MDA Interface	-0.017	±0.165	-0.057	±0.140	0.0	±0.135	
S193/DA Interface	0.0	±0.300	0.0	±0.265	0.0	±0.200	
S194/MDA Interface	-0.006	±0.165	0.059	±0.135	0.0	±0.120	

APPENDIX C

# SKYLAB VEHICLE/EXPERIMENT COMPATIBILITY ASSESSMENT

This appendix demonstrates the use of the compatibility assessment procedure by presenting a portion of the Skylab vehicle/experiment compatibility analysis. The compatibility analyses for EREP, other selected experiments, and the ATM and S020 simultaneous operation case are included. The attitude control information and experiment misalignment were obtained from documentation or supplied by the appropriate technical specialists [12].[4,5] The vehicle misalignments (M_V), experiment misalignments (M_E), and attitude control errors (A) were assumed to be 3σ values and root sum squared to obtain the total pointing capability. The appropriate equation was then used to test for compatibility.

A typical Z-LV maneuver profile is described in Figure C-1. Tables C-1, C-2, and C-3 provide the compatibility assessment for different times in the maneuver profile. The pointing compatibility assessment for selected corollary experiments is shown in Table C-4.

NOTES:

1. Experiment has a sighting device so equation (1) must be satisfied, i.e., $M_V + M_E + A \leq E_{FOV}$ or C. In this case, the experiment is adjustable so C is replaced by the range of possible adjustment.

---

4. Melvin Brooks, Pointing Accuracy for Extended Z-LV EREP Passes, MSFC memorandum S&E-ASTR-SG-105-72, Marshall Space Flight Center, Marshall Space Flight Center, Ala., July 10, 1972.

5. Carlos C. Hagood, Attitude Pointing Capability for EREP and Corollary Experiments Meeting Minutes, MSFC memorandum S&E-CSE-A-71-494, Marshall Space Flight Center, Marshall Space Flight Center, Ala., Oct. 26, 1971.
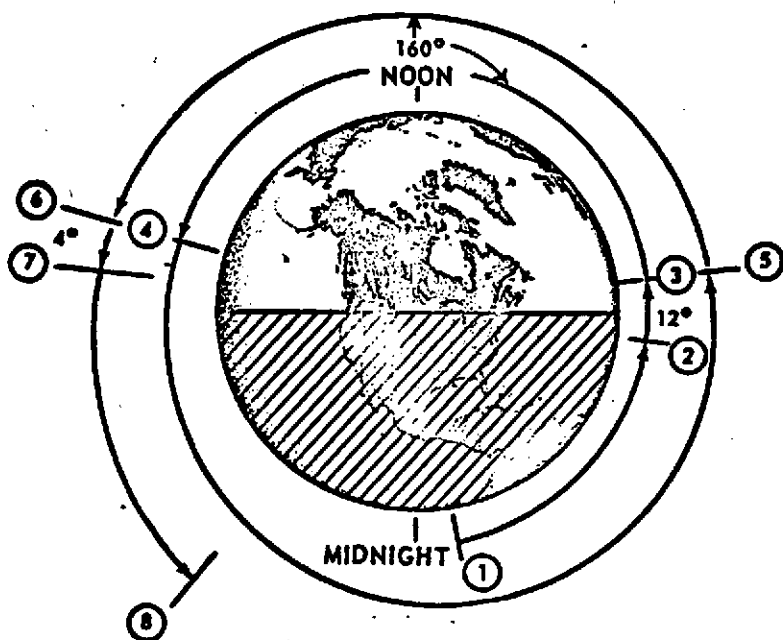
1. Start maneuver to Z-LV:
   12 deg after midnight for beta = 0 deg
   (maneuver required 76 orbital deg)
   2 deg after midnight for beta = -65 deg
   (maneuver required 86 orbital deg)

2. End maneuver:
   Allow 3 min or ~ 12 deg for stabilization prior to data take

3. Start first 160 deg data take centered about noon

4. End first 160 deg data take:
   Remain in Z-LV until next data take

5. Start second 160 deg data take centered about noon

6. End second data take:
   Allow 1 min or ~ 4 deg prior to starting back to solar inertial

7. Start maneuver back to solar inertial —
   assume same "T" as going into Z-LV.

8. End maneuver:
   10 deg before midnight for beta = -65 deg
   20 deg before midnight for beta = 0 deg.

Figure C-1. Z-LV maneuver profile.

TABLE C-1. EREP POINTING COMPATIBILITY ASSESSMENT — END FIRST DATA TAKE

Expt. No.	Experiment Requirement (P)	Vehicle Capability(Degrees (°) Rotation About the Specified Axis)												Results
		Vehicle Misalignment			Expt. Misalignment			Attitude Control Error			RSS Total (3σ)			
		M_{vx}	M_{vy}	M_{vz}	M_{ex}	M_{ey}	M_{ez}	A_x	A_y	A_z	X	Y	Z	
S190A	Vehicle Side of Vehicle/Experiment Interface Pointed to ± 2° of NADIR	0.023 ±0.727	0.038 ±0.630	0.0 ±0.242	±0.5	±0.5	±0.5	±0.851	±0.623	±0.854	0.023 ±1.226	0.038 ±1.017	0.0 ±1.019	Vehicle Capability < experiment requirements. Therefore, experiments and vehicle are compatible.
S190B	Experiment Side of Interface Pointed to ± 2.5° of Nadir.	1.883 ±1.305	-0.027 ±1.005	0.0 ±0.810							1.883 ±1.636	-0.027 ±1.284	0.0 ±1.279	
S191		-0.121 ±0.736	-0.191 ±0.676	0.0 ±0.244							-0.121 ±1.231	-0.191 ±1.046	0.0 ±1.020	
S192		-0.017 ±0.737	-0.057 ±0.628	0.0 ±0.254	±0.031	±0.024	±0.5				-0.017 ±1.126	-0.057 ±0.885	0.0 ±1.022	
S193		0.0 ±0.759	0.0 ±0.688	0.0 ±0.267	±0.15	±0.15	±0.15				0.0 ±1.150	0.0 ±0.940	0.0 ±0.908	
S194		-0.006 ±0.742	0.059 ±0.625	0.0 ±0.250	±0.1	±0.1	±0.1				-0.006 ±1.134	0.059 ±0.888	0.0 ±0.895	

TABLE C-2. EREP POINTING COMPATIBILITY ASSESSMENT — START SECOND DATA TAKE

Expt. No.	Experiment Requirement (P)	Vehicle Capability(Degrees (°) Rotation About the Specified Axis)												Results
		Vehicle Misalignment			Expt. Misalignment			Attitude Control Error			RSS Total (3σ)			
		M_{vx}	M_{vy}	M_{vz}	M_{ex}	M_{ey}	M_{ez}	A_x	A_y	A_z	X	Y	Z	
S190A	Vehicle Side of Vehicle/Experiment Interface Pointed to ± 2° of Nadir	0.023 ±0.727	0.038 ±0.630	0.0 ±0.242	±0.5	±0.5	±0.5	±1.440	±1.032	±1.442	0.023 ±1.689	0.038 ±1.308	0.0 ±1.546	Vehicle capability < experiment requirements. Therefore, experiments and vehicle are compatible
S190B	Experiment Side of Interface Pointed to ± 2.5° Nadir	1.883 ±1.305	-0.027 ±1.005	0.0 ±0.810							1.883 ±2.007	-0.027 ±1.524	0.0 ±1.728	
S191		-0.121 ±0.736	-0.191 ±0.676	0.0 ±0.248							-0.121 ±1.693	-0.191 ±1.331	0.0 ±1.547	
S192		-0.017 ±0.737	-0.057 ±0.628	0.0 ±0.254	±0.031	±0.024	±0.5				-0.017 ±1.618	-0.057 ±1.208	0.0 ±1.548	
S193		0.0 ±0.759	0.0 ±0.698	0.0 ±0.267	±0.15	±0.15	±0.15				0.0 ±1.635	0.0 ±1.255	0.0 ±1.474	
S194		-0.006 ±0.742	0.059 ±0.625	0.0 ±0.250	±0.1	±0.1	±0.1				-0.006 ±1.624	0.059 ±1.211	0.0 ±1.468	

TABLE C-3. EREP POINTING COMPATIBILITY ASSESSMENT — END SECOND DATA TAKE

Expt. No.	Experiment Requirement (P)	Vehicle Misalignment			Expt. Misalignment			Attitude Control Error			RSS Total (3σ)			Results
		M_{vx}	M_{vy}	M_{vz}	M_{ex}	M_{ey}	M_{ez}	A_x	A_y	A_z	X	Y	Z	
S190A	Vehicle Side of Vehicle/Experiment Interface Pointed to ± 2° of Nadir.	0.023 ±0.727	0.038 ±0.630	0.0 ±0.242	±0.5	±0.5	±0.5	±1.920	±1.352	±1.922	0.023 ±2.113	0.038 ±1.573	0.0 ±2.001	Vehicle capability < experiment requirements. Therefore, experiments and vehicle are compatible.
S190B	Experiment Side of Interface Pointed to ± 2.5° of Nadir	1.883 ±1.305	-0.027 ±1.005	0.0 ±0.810							1.883 ±2.375	-0.027 ±1.757	0.0 ±2.145	
S191		-0.121 ±0.736	-0.191 ±0.676	0.0 ±0.248							-0.121 ±2.116	-0.191 ±1.591	0.0 ±2.001	
S192		-0.017 ±0.737	-0.057 ±0.628	0.0 ±0.254	±0.031	±0.024	±0.5				-0.017 ±2.057	-0.057 ±1.491	0.0 ±2.002	
S193		0.0 ±0.759	0.0 ±0.688	0.0 ±0.267	±0.15	±0.15	±0.15				0.0 ±2.066	0.0 ±1.524	0.0 ±1.946	
S194		-0.006 ±0.742	0.059 ±0.625	0.0 ±0.252	±0.1	±0.1	±0.1				-0.006 ±2.059	0.059 ±1.493	0.0 ±1.941	

Vehicle Capability(Degrees (°) Rotation About the Specified Axis)

TABLE C-4. POINTING COMPATIBILITY ASSESSMENT FOR SELECTED COROLLARY EXPERIMENTS

Expt. No.	Expt. Requirement FOV How Pointed	Accuracy (°)	Vehicle Capability(Degrees (°) Rotation About the Specified Axis) Vehicle Misalignment M_{vx}	M_{vy}	M_{vz}	Expt. Misalignment M_{ex}	M_{ey}	M_{ez}	Attitude Cont Error ⚠ A_x	A_y	A_z	RSS Total (3σ) X	Y	Z	Results
S019	FOV - 7° Observer Sighting, Articulate Mirror	±0.5	1.883 ±1.065	-0.217 ±0.825	0.0 ±0.559	±0.100	±0.100	±0.100	±0.1°	±0.1°	±0.1°	1.883 ±1.074	-0.217 ±0.837	0.0 ±0.577	Compatible. See Note △a
S020	FOV - 2° Observer Sighting, Bias Vehicle △2	±0.25	-0.150 ±1.065	-0.163 ±0.825	0.0 ±0.559	±0.133	±0.133	±0.133				-0.150 ±1.078	-0.163 ±0.842	0.0 ±0.583	Compatible. See Note △b
S063	FOV - 12° Observer Sighting & Adjustable Camera Mount	±0.5 Post-flight knowledge										-0.150 ±1.181	±0.970	±0.757	Compatible. See Note △c
T025	FOV - 8° Observer Sighting, Bias Vehicle △2	±0.25				±0.100	±0.100	±0.100				-0.150 ±1.074	±0.837	±0.577	Compatible. See Note △d
T027	No Observer Sighting	±0.5 Post-flight knowledge				±2.0°	±2.0°	±2.0°				-0.150 ±2.268	±2.166	±2.079	Incompatible. See Note △e

△1 Vehicle Attitude Hold Capability ±0.1° Day ±0.2° Night

△2 Vehicle Attitude Bias Capability ±4°

E_{FOV} = 7 deg < adjustment capability

M_V + M_E + A about the worst-case axis

= 1.883 deg ± 1.074 deg = 2.957 deg maximum .

Since M_V + M_E + A ≤ E_{FOV} and attitude hold capability < pointing accuracy requirement, the experiment and vehicle are compatible.

2. M_V + M_E + A ≤ E_{FOV} or C.

In this case E_{FOV} (= 2 deg) < C (= ± 4 deg) .

M_V + M_E + A about the worst-case axis

= -0.150 deg ± 1.078 deg = -1.228 deg maximum.

Since M_V + M_E + A ≤ E_{FOV} and attitude hold capability < point accuracy requirement, compatibility exists.

3. This experiment has pointing accuracy requirement for postflight knowledge. In this case, the experiment can be adjusted and the pointing determined in-flight. However, neither the range of adjustment nor C are important in equation (1). As long as the target can be located through the sighting device, the postflight knowledge requirement is satisfied.

E_{FOV} = 12 deg.

$$M_V + M_E + A \text{ about the worst-case axis}$$

$$= -0.150 \text{ deg} \pm 1.181 \text{ deg} = -1.331 \text{ deg maximum.}$$

$$M_V + M_E + A \leq E_{FOV} \quad .$$

In addition, the attitude hold capability plus sighting uncertainties < pointing accuracy requirement. Thus, the vehicle and experiment are compatible.

4. Experiment has a sighting device. In equation (1),

$$C \ (= \pm 4 \text{ deg}) = E_{FOV} \ (= 8 \text{ deg}) \quad .$$

$$M_V + M_E + A \text{ about the worst-case axis}$$

$$= -0.150 \text{ deg} \pm 1.074 \text{ deg} = 1.224 \text{ deg maximum.}$$

$$M_V + M_E + A \leq E_{FOV} \text{ or } C \quad .$$

In addition, the attitude hold capability < pointing accuracy requirement. Therefore, vehicle/experiment compatibility exists.

5. Experiment has no sighting device, so equation (2) must be satisfied, i.e., $M_V + M_E + A \leq P.$

$$M_V + M_E + A \text{ about the worst-case axis}$$

$$= -0.150 \text{ deg} \pm 2.268 \text{ deg} = -2.418 \text{ deg maximum} \quad .$$

Since this pointing accuracy requirement is for postflight knowledge, the M_V could be reduced considerably by running another experiment with a sighting device to determine the actual M_V. However, $M_V + M_E + A$ would still be >P. Thus, the experiment and vehicle are incompatible.

The procedure for simultaneous operation of the S020 (Solar SAL) and ATM experiment(s) is described in Figure C-2. This procedure was to be accomplished by having one crewman control the SWS attitude from the ATM while another determined the required maneuver by using the S020 sighting device. For compatibility in this case the misalignment of the ATM experiment(s) and the S020 must be less than ±1.30 deg about the X and Y SAS-axes from Figure C-2. Rotation about the Z-axis has no effect.

The misalignment of ATM experiment S052 and the ATM basic datum is as follows:

about X   ± 0.050 deg

about Y   ± 0.050 deg

These misalignments, when combined with vehicle and S020 misalignments from Appendix B, yield the following vehicle capability associated with a 99.7-percent probability:
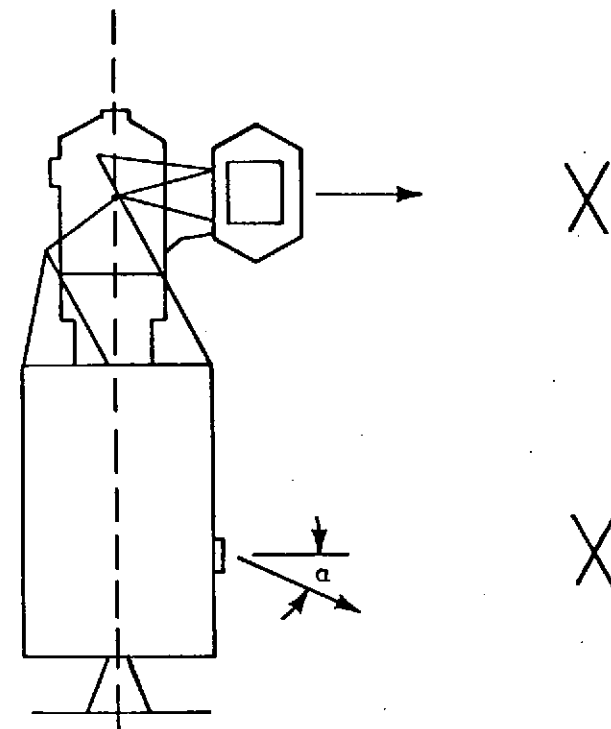
about X   -0.150 deg ± 1.094 deg

about Y   -0.163 deg ± 0.874 deg

Even if a maximum uncertainty error exists in the same direction as the bias, the resulting error is less than the experiment requirement (±1.30 deg). Thus, simultaneous operation is possible.
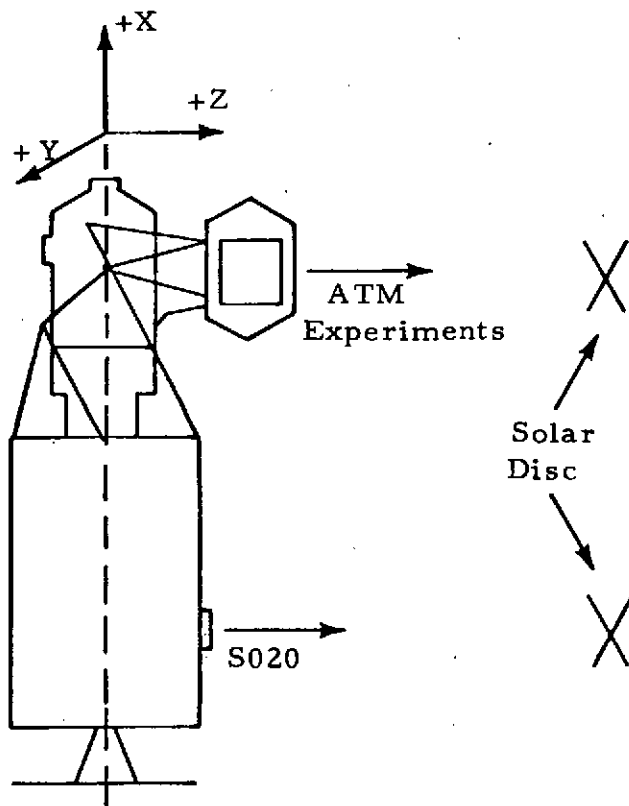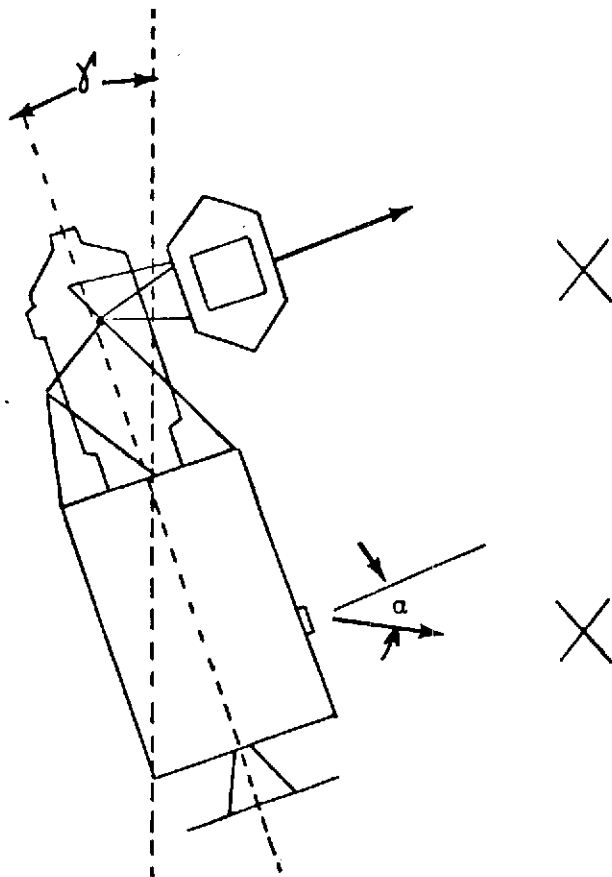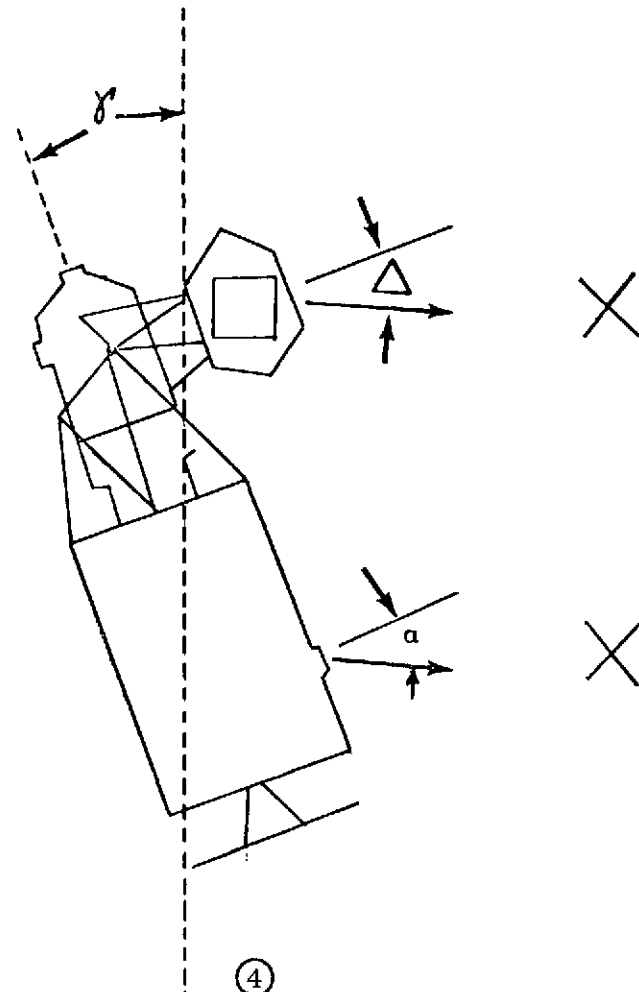
Figure C-2. S020/ATM simultaneous operations procedure.

③

Bias SWS by γ = α

$\left| \gamma_{max} \right|$ = $4°$

④

Rotate ATM Canister by $\Delta = \gamma$ = α

$\left| \Delta_{max\ usable} \right|$ = $1.30°$

Figure C-2. S020/ATM simultaneous operations procedure (concluded).

APPENDIX D

COMPARISON OF SKYLAB MISALIGNMENT PREDICTIONS AND SKYLAB ALIGNMENT DATA

The misalignment data from the Skylab missions are in the form of coordinate system transformations. The various transformations and transformation computation procedures are described in MSC and JSC Internal Notes.[6,7,8] The Skylab transformation data from two MSFC documents[9,10] are as follows.

1. CSM-to-ATM

SL-2	SL-3	SL-4
α = 146.60 deg	α = 146.3 deg	α = 144.49 deg
β = 180.2 deg	β = 180.2 deg	β = 180.05 deg
γ = 000.2 deg	γ = 000.1 deg	γ = 000.14 deg

6. Final Skylab Pointing Control Mission Techniques, MSC Internal Note MSC-07220, Johnson Space Center, Houston, Tex., Oct. 11, 1972.

7. Instrument Definition Table for the Attitude/Pointing Subsystem of the Activity Scheduling Program, Rev. 1, JSC Internal Note 72-FM-130, MSC 06866, Johnson Space Center, Houston, Tex., May 17, 1973.

8. MOPS Program Requirements: Skylab Cluster Coordinate Determination, MSC Internal Note 71-FM-419, MSC-05248, Johnson Space Center, Houston, Tex., Dec. 10, 1971.

9. Stephen G. Bales, Reply to DRF H-00790-T, MSFC memorandum MO-I-DRF-1444, Return of Data Request Form to Originator, Marshall Space Flight Center, Marshall Space Flight Center, Ala., Nov. 14, 1973.

10. R. Stone, Addendum to Reply to DRF Control No. H-00790-T, Marshall Space Flight Center, Marshall Space Flight Center, Ala., Nov. 26, 1973.

where

$$\alpha = 180 \text{ deg} - \text{OGA},$$

$$\beta = \text{IGA},$$

$$\gamma = \text{MGA},$$

and OGA, IGA, and MGA are the Euler angles (X, Y, Z respectively) that relate the CSM coordinate system to the ATM coordinate system.

Nominal values for α, β, and γ are 145 deg, 180 deg, and 0 deg, respectively.

2. IU-to-ATM

$$\alpha = +0.050 \text{ deg},$$

$$\beta = +0.050 \text{ deg},$$

$$\gamma = +0.210 \text{ deg},$$

where α, β, and γ are the Euler angles (X, Y, Z respectively) that relate the IU and ATM coordinate systems.

Nominal values for α, β, and γ are all 0 deg. This transformation was computed once and not updated.

3. CSM Docking Angle

SL-2	SL-3	SL-4
33.515 deg	33.830 deg	35.81 deg

Nominal CSM docking angle = 35 deg.

4. S019 to ATM

The predicted value of this transform was

$$\phi = 91.907 \text{ deg},$$

$$\theta = 45.00 \text{ deg},$$

$$\phi' = 89.962 \text{ deg},$$

56

where ϕ, θ, ϕ' are the Euler angles in X, Y, Z order which relate the S019 coordinate system and the ATM coordinate system.

The flight data indicated that these values were correct. This transform was computed during the SL-2 mission and was not updated.

5. S020 to ATM

This transformation could not be determined, since the Solar SAL could not be used for experiments.

6. MDA to ATM

α = -0.120 deg,

β = -0.135 deg,

γ = +0.097 deg,

where α, β, and γ are the Euler angles (X, Y, Z respectively) that relate the ATM and MDA coordinate systems.

The transformation was determined during the SL-2 mission and was not updated.

These transformations were determined using the various Skylab attitude control systems and/or experiments. Thus, the transformations include the applicable control system and/or experiment uncertainties in addition to the vehicle misalignments. This makes a direct comparison of actual and predicted misalignments difficult. The best indication of the accuracy of the misalignment predictions would have been provided by the ATM-to-S020 transformation, since no control system uncertainties would have been included. However, because of mission events, this transformation was not performed.

The analyses in Appendix B were primarily concerned with the misalignment of a given control system and experiment. The transformations primarily concern the misalignment of different control systems. Thus, some additional analyses were performed using the alignment components from Appendix A and the technique described in Appendix B. The results are compared with selected transformation data in Table D-1. This comparison indicates that the misalignment predictions were generally conservative. Although the predictions were conservative by as much as an order of magnitude in some cases, they would still be useful as a mission planning tool for future programs.

TABLE D-1. COMPARISON OF SKYLAB TRANSFORMATION DATA AND VEHICLE MISALIGNMENT PREDICTIONS

Transformation	Results* (Deg.)			Vehicle Misalignment Case	Prediction (Deg. -3σ)		
	X	Y	Z		X	Y	Z
IU-to-ATM	0.050	0.050	0.210	ST-124 to ATM Basic Datum	0.0 ±0.510	0.175 ±0.585	0.0 ±0.325
S019-to-ATM	1.869	—	—	Anti-Solar SAL to ATM Basic Datum	1.883 ±1.305	-0.027 ±1.005	0.0 ±0.810
MDA-to-ATM	-0.120	-0.135	0.097	MDA Basic Datum to ATM Basic Datum	0.0 ±0.380	0.075 ±0.465	0.0 ±0.105

*Transformation results include applicable control system errors in addition to vehicle misalignments.

REFERENCES

1. Bower, Ralph E.: Skylab Experiment Accuracy Analysis, MMC Report ED-2002-1240, Rev. A, Martin Marietta Corp., Denver, June 25, 1971.

2. MSFC Drawing No. 10M03786, Rev. G, ATM Alignment Parameters for ATM-A, Marshall Space Flight Center, Huntsville, Ala., November 1968.

3. MSFC Drawing 10M03736, Rev. C, ATM-A Alignment Control Drawing, Marshall Space Flight Center, Huntsville, Ala., August 1971.

4. MSFC Drawing No. 13M20726, Rev. A, AM(DA) (PS)/ATM/MDA Mechanical Interface Control Drawing, Marshall Space Flight Center, Huntsville, Ala., November 1971.

5. MSFC Drawing No. 10M03933, Skylab A-AM/FAS/DA Alignment Control Drawing, Marshall Space Flight Center, Huntsville, Ala., April 1971.

6. MSFC Drawing No. 10M04149, Rev. B, Instrument Unit Saturn V Alignment Control, Marshall Space Flight Center, Huntsville, Ala., April 1964.

7. International Business Machines (IBM) Drawing 6009033, Rev. H; Specification, Instrument Unit Saturn V Alignment Control; Huntsville, Ala., April 1968.

8. MSFC Drawing No. 10M03931, Skylab A-MDA Alignment Control Drawing, Marshall Space Flight Center, Huntsville, Ala., July 1970.

9. MSFC Drawing No. 13M12201, S190/MDA Interface Control Document, Marshall Space Flight Center, Huntsville, Ala., May 1970.

10. MSFC Drawing No. 13M07398, S193/AM-DA Mechanical Interface Control Drawing, Marshall Space Flight Center, Huntsville, Ala., Dec. 28, 1970.

11. MSFC Drawing No. 13M20979, Rev. B, CSM to MDA Physical Requirements Interface Control Document, Marshall Space Flight Center, Huntsville, Ala., July 31, 1972.

12. Skylab Operational Data Book. Vol. I, Experiment Performance Data, Johnson Space Center, NASA, Houston, Tex., Oct. 12, 1972.

APPROVAL

VEHICLE MISALIGNMENT PREDICTION AND VEHICLE/EXPERIMENT POINTING COMPATIBILITY ASSESSMENT

By J. D. Hoverkamp

The information in this report has been reviewed for security classification. Review of any information concerning Department of Defense or Atomic Energy Commission programs has been made by the MSFC Security Classification Officer. This report, in its entirety, has been determined to be unclassified.
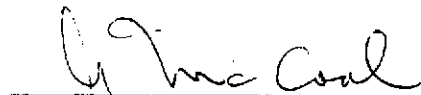
This document has also been reviewed and approved for technical accuracy.

W. C. ASKEW
Chief, Mission Development Branch

T. P. ISBELL
Chief, Mechanical and Crew Systems Integration Division

A. A. McCOOL, JR.
Acting Director, Astronautics Laboratory